

RICE UNIVERSITY

**Parameter Estimation in Mathematical Models of Lung
Cancer**

by

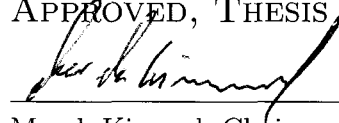
Deborah L. Goldwasser

A THESIS

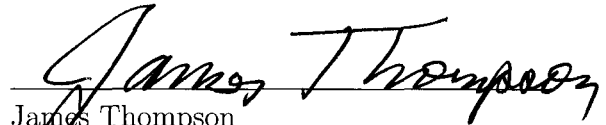
SUBMITTED IN PARTIAL FULFILLMENT OF THE
REQUIREMENTS FOR THE DEGREE

Doctor of Philosophy

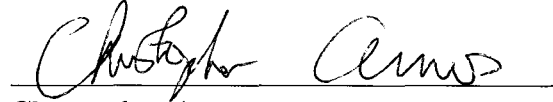
APPROVED, THESIS COMMITTEE:



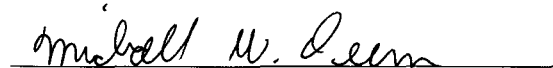
Marek Kimmel, Chairman
Professor of Statistics, Rice University



James Thompson
Noah Harding Professor of Statistics, Rice
University



Christopher Amos
Professor of Epidemiology, Bioinformatics
and Computational Biology, University of
Texas M.D. Anderson Cancer Center



Michael Deem
John W. Cox Professor of Biochemical
and Genetic Engineering, Rice University

HOUSTON, TEXAS

AUGUST, 2009

UMI Number: 3421184

All rights reserved

INFORMATION TO ALL USERS

The quality of this reproduction is dependent upon the quality of the copy submitted.

In the unlikely event that the author did not send a complete manuscript and there are missing pages, these will be noted. Also, if material had to be removed, a note will indicate the deletion.



UMI 3421184

Copyright 2010 by ProQuest LLC.

All rights reserved. This edition of the work is protected against unauthorized copying under Title 17, United States Code.



ProQuest LLC
789 East Eisenhower Parkway
P.O. Box 1346
Ann Arbor, MI 48106-1346

Abstract

Parameter Estimation in Mathematical Models of Lung Cancer

by

Deborah L. Goldwasser

The goal of this thesis is to improve upon existing mathematical models of lung cancer that inform policy decisions related to lung cancer screening. Construction of stochastic, population-based models of lung cancer relies upon careful statistical estimation of biological parameters from diverse data sources. In this thesis, we focus specifically on two distinct aspects of parameter estimation. First, we propose a model-based framework to estimate lung cancer risk due to repeated low-dose radiation exposures using the two-stage clonal expansion (TSCE) model. We incorporate the TSCE model into a Bayesian framework and formulate a likelihood function for randomized screening data. The likelihood function depends on model-based risk correlates and effectively penalizes parameter values that correspond to model-based contradictions. The net result is that both the sensitivity and specificity of parameter estimation relating to excess lung cancer risk is increased. This methodology is applied to data from the Mayo Lung Project and estimates of 10-year excess lung cancer risk as a function of age at enrollment and number of screens are derived. Second, we describe a new statistical approach aimed at improving our understanding of the natural course of lung cancer. Specifically, we are interested in evaluating the evidence for, or against, the bi-modal hypothesis which proposes that lung cancers are of two

categories, either slow-growing and non-invasive cancers (tending to over-diagnosis) or rapidly-growing and highly aggressive. We represent the growth trajectory of lung tumors using the evolutionary parameters of cancer stem cell branching fraction (f) and cell mutation rate (μ). While concern over widespread implementation of lung cancer screening has focused primarily on the extent of over-diagnosis, these results are consistent with the presence of a high percentage of rapidly-growing, aggressive cancers.

Acknowledgements

I would like to first thank my mentor and thesis committee chair, Professor Marek Kimmel of Rice for his commitment to my thesis project, willingness to always help, and for his support of as well as improvement of my ideas. I would furthermore like to thank my thesis committee, Professors James Thompson and Michael Deem of Rice and Professor Christopher Amos of U.T. MD Anderson Cancer Center. Their comments and support are much appreciated.

I am also very grateful for funding support from the NCI cancer prevention fellowship awarded by the University of Texas M.D. Anderson Cancer Center's Cancer Prevention Program, R25 CA57730, Robert M. Chamberlain, Ph.D., Principal Investigator and Shine Chang, Ph.D.. I could not have completed this thesis without the data resources that have been generously provided by Pamela Marcus, PhD. of the National Cancer Institute (NCI), the I-ELCAP investigators of New York's Weill Cornell Medical College, the Mayo Clinic and the NCI CISNET research consortium. I would also like to thank Dr. Andrei Rodin and Mr. Grigoriy Gogoshin of the U.T. School of Public Health for allowing me the use of their super-computer to run my simulations in parallel.

Contents

Abstract	ii
Acknowledgements	iv
1 Introduction	1
1.1 Overview: Lung Cancer Screening	1
1.2 Overview: Excess Lung Cancer Risk Estimation	4
1.3 Overview: Tumor Progression Modeling	5
1.4 Data-Sets	7
1.4.1 Mayo Lung Project	7
1.4.2 Mayo CT	9
1.4.3 International Early Lung Cancer Action Program (I-ELCAP)	11
1.4.4 Lung Screening Study (LSS)	12
2 Excess Lung Cancer Risk Estimation	14
2.1 Mathematical Models of Carcinogenesis	14
2.2 Atomic Bomb Survivor Data	15
2.3 Mathematical Model of Natural Course of Lung Cancer	18
2.4 Framework for Estimating Lung Cancer Risk in the MLP	19
2.4.1 Mathematical Formulation of the Model	21
2.4.2 Likelihood-Based Estimation of the Model Parameters	22

2.4.3	Simulations Using the Estimated Distribution of k'_i and Calculation of Lung Cancer Excess Risk	24
2.5	Results	25
2.5.1	Model Calibration and Stochastic Variability	25
2.5.2	Maximum Likelihood Estimation of Excess Risk	25
2.5.3	Simulation of the Natural Course of Lung Cancer Assuming Excess Risk and Stochastic Variability	26
2.6	Discussion and Conclusions	27
3	Tumor Progression Modeling	31
3.1	Introduction	31
3.2	Relationship Between Tumor Size and Tumor Stage	32
3.2.1	Cancer Registry Data	32
3.2.2	Lung Cancer Screening Data	34
3.3	Lung Tumor Growth Rate and Over-diagnosis	36
3.4	Models of Lung Cancer Progression	37
3.5	Methods and Models	39
3.5.1	Simulation Analysis of Mayo CT Data	39
3.5.2	Homogeneity Analysis of Mayo CT and Mayo Lung Project Data	41
3.5.3	Data Visualization and Clustering of Mayo CT and Mayo Lung Project Data Based on Branching Fraction (f) and Cell Mutation Rate (μ)	42
3.6	Results	45
3.6.1	Simulation Analysis of Mayo CT Data	45
3.6.2	Homogeneity Analysis of Mayo CT and Mayo Lung Project Data	46
3.6.3	Data Visualization and Clustering of Mayo CT and Mayo Lung Project Data Based on Branching Fraction (f) and Cell Mutation Rate (μ)	46
3.7	Discussion	48

4	Summary and Future Directions	51
5	Tables and Figures	53
	Bibliography	68

Chapter 1

Introduction

1.1 Overview: Lung Cancer Screening

Lung cancer has the second highest incidence for both genders, second only to prostate cancer in men and breast cancer in women. Because lung cancer is primarily detected at an advanced stage, it is responsible for the largest number of cancer deaths in both men and women [58] in the U.S. and most advanced countries. A key focus of cancer prevention efforts has been centered on smoking cessation. However, because former smokers remain indefinitely at an increased lung cancer risk, smoking cessation programs have had only a limited effect on lowering lung cancer mortality. There is a continued need for effective secondary prevention in the form of early detection and early treatment. The paradigm in the early detection of lung cancer is that the earlier the disease is detected, the less likely it is to have spread to distal regions of the body, and the higher the curability and survival rate.

Despite the theoretical advantages of early detection, in practice lung cancer screening trials have produced ambiguous results. In particular, they have failed to show a mortality benefit attributable to screening in the context of a randomized clinical trial. The Mayo Lung Project (MLP) was the most extensive randomized clinical

trial designed to evaluate a mortality benefit attributable to screening by chest x-ray. However, in the MLP, despite the detection of a higher number of early-stage cancers in the screening arm, there were more lung cancer deaths in the screening arm than the control arm [18, 19]. After more than twenty years of follow-up, there were a greater number of both lung cancers and lung cancer deaths among screened participants [40, 41]. Computed tomography (CT) may prove superior to chest x-ray as a means of early detection. A study appearing in the *New England Journal of Medicine* reported that CT screening resulted in the estimated 10-year survival of 88% of Stage I-detected cancers [30]. On the other hand, there are potential risks associated with screening resulting from repeated radiation exposures and from unnecessary surgical interventions. Presently, no national cancer advisory source is willing to endorse lung cancer screening in the broader population [32, 4].

In order to predict the impact of an early detection program in lung cancer, we need a quantitative understanding of both the disease's natural course and of the risks associated with screening. The biology of lung cancer progression may limit the effectiveness of early detection methods. A high prevalence of very aggressive cancers that metastasize rapidly at a small size and/or very slow-growing tumors can limit the effectiveness of a screening program within a targeted population. The latter phenomenon of detecting slow-progressing cancers that are unlikely to shorten a patient's life expectancy is commonly referred to as "over-diagnosis". In the first scenario, the time window for early detection is too short to be practically implemented and in the second scenario, early detection does not improve survival because the tumor was not life-threatening.

Over-diagnosis has been frequently cited as an explanation to the seemingly paradoxical findings of improved survival of screen-detected cases in the Mayo Lung Project [7, 41, 57]. However, a pathologic review of cases detected in the MLP confirmed the

histologic diagnosis of cancer in all cases it studied although a higher rate of carcinoma in situ detected in the screening arm was noted [11]. Other studies indicate that the power of the MLP may have been lower than initially planned, and that the initial findings of the MLP were not inconsistent with a model of moderately aggressive tumor progression and a modest mortality benefit [15, 24]. The inconclusive findings of the MLP have led to debate as to whether randomized clinical trials are an efficient way to study the benefits of screening [45, 50].

In lieu of a high degree of over-diagnosis, another distinct aspect of cancer biology may also explain the failures of lung cancer screening trials to date, namely the micro-evolution of pre-malignant cells in the lung. Mathematical models of lung cancer that describe the growth of pre-malignant cells have been shown to be consistent with age and exposure-dependent patterns of lung cancer risk in epidemiologic datasets [44, 46]. This same population of pre-malignant cells may likewise be susceptible to malignant transformation due to radiation exposures incurred during screening. The survival advantage of early detection may be negated if the total lung cancer incidence rate in screened arm participants is elevated.

The failure to demonstrate a mortality benefit in lung cancer screening trials has been near-unanimously attributed to over-diagnosis, without considering evidence supporting competing hypotheses. Using the statistical estimation techniques outlined in this thesis, we will focus separately on the estimation of excess lung cancer risk attributable to low-dose radiation exposure in individuals with long prior exposures to cigarette smoke and on the estimation of the proportion of aggressive, rapidly-growing and over-diagnosed lung cancers in the population.

1.2 Overview: Excess Lung Cancer Risk Estimation

In order to estimate the excess lung cancer risk attributable to repeated screening by chest x-ray, we modify a two-stage clonal expansion (TSCE) model and estimate excess lung cancer risk using a Bayesian framework. The advantage of this approach is the ability to incorporate information on risk correlates which are specific to radiation-induced lung cancer risk. In contrast to the proportional hazards model, the TSCE model predicts a correlation of excess lung cancer risk with age at exposure and exposure frequency. A key feature of the long-term follow-up data in the MLP is that excess lung cancer risk in screened arm participants is correlated with the number of screens received and age at enrollment. By parameterizing our estimation methodology in accordance with the TSCE model, we increase the power to detect an excess risk of radiation exposure compared to the proportional hazards method. Whereas the original report of the long-term follow-up MLP data found that the increase in lung cancer deaths was not significant, we find that excess lung cancer risk in the MLP is significantly higher among screened arm participants versus control arm participants ($p=0.002$).

We believe that this approach has broader implications beyond the scope of this study. While the number of patients recruited for a given clinical trial may be limited, the range of data collected for each patient is ever-increasing. This represents the classical "small n, large p" problem. A model-based framework for estimation imposes constraints on the parameter space of solutions, which is reflected in the likelihood function. Parameter values that are inconsistent with the model predictions for a given data-set will be penalized more strongly than if a model-based estimation framework was not used. Ultimately, this increases the power to assign statistical significance to a given parameter value ($p < 0.05$) when risk correlates are consis-

tent with model assumptions, but also increases the ability to reject a parameter as statistically significant when the risk correlates violate the model assumptions. Both sensitivity and specificity are thereby improved simultaneously. The drawback of such an approach is that the model framework must be well-validated and based on a priori biological knowledge. In the case of a flexible version of the TSCE model in lung cancer, this condition is satisfied.

1.3 Overview: Tumor Progression Modeling

We evaluate the ability of our existing stochastic model of lung cancer progression, calibrated to incidence data from the MLP, to explain findings from annual repeat screening in the Mayo CT screening trial. The Mayo CT trial found 66 cancers, of which there were 15 incidence non-small cell lung cancers found in males, the cohort comparable to the MLP. Despite the small size of the data-set, there were a significantly greater percentage of advanced-stage cancers appearing during the annual-repeat screens than predicted by the model. The radiologic size of advanced-stage cancers in the Mayo CT study was smaller on average than the early-stage cancers detected by chest x-ray, with implications for evaluating a size-driven model of lung cancer progression. The large size of early-stage cancers in the MLP compared to the small advanced cancers in the Mayo CT challenges the notion that large early-stage cancers progress to advanced-stage disease. We test whether both sets of data can be reconciled by a single statistical model of tumor growth and progression. In the first model, we assume tumors grow exponentially with a size at stage transition governed by the Gaussian distribution, independent of growth rate. We reject homogeneity of the data based on a significant difference between the mean size at stage transition between the two data-sets. Next, we define a statistical model governed by a multi-type Galton-Watson branching process representing tumor growth

and stage transition as a function of two evolutionary parameters, namely, the cancer stem cell branching fraction (f) and cell mutation rate (u). We simulate a likelihood distribution for each cancer case reflecting tumor size, its prior history, and stage at detection. We again reject homogeneity of the two data-sets based on a model in which cancers from the MLP and Mayo CT derive from a common distribution governed by a single parameter combination of f and u . However, when we cluster the MLP cancers based on a concordance matrix representing similarity of likelihoods, we find that the advanced-stage cancers detected in the Mayo CT are consistent with a unique cluster of advanced-stage MLP cancers, but not distinct clusters representing early-stage cancers.

Our analysis lends support to a bi-modal model of tumor progression, in which some lung tumors progress to an advanced stage rapidly whereas others progress slowly and may reach modest sizes without transitioning to advanced-stage disease. The analysis methods we describe and apply depend upon lung cancer data detected by different screening modalities. CT can identify cancers early in the natural course of lung cancer due to its low size at detection threshold and high sensitivity. Therefore, data from CT screening trials (both single-arm and randomized) detected at annual repeat screens represent a unique opportunity to evaluate the size and frequency of advanced-stage cancers, potentially at smaller sizes than previously ever recorded. Additional comparisons of data from CT screening with data from cancer registry and chest x-ray trials may prove highly informative to models of lung cancer natural course because they provide a window into different time points of disease (early and late) progression. Our methodology may be particularly applicable to data from the National Lung Screening Trial (NLST) when it becomes available. The NLST is a randomized clinical trial comparing chest x-ray to CT in reducing lung cancer mortality. Additional data on chest x-ray screening outcomes from the Prostate, Lung, Colorectal, and Ovarian Cancer Screening Trial (PLCO) are forthcoming as well.

1.4 Data-Sets

1.4.1 Mayo Lung Project

The MLP, initiated in 1971 and completed on July 1, 1983, recruited 10,933 male smokers over the age of 45 years to receive a baseline chest radiography screen. Of those initially recruited in the MLP, 91 prevalence cases, i.e. patients who tested positively for lung cancer on the initial screen, were identified and followed separately. Of those that remained, 9,211 satisfactorily passed other entry criteria and were randomized into two groups: a screening and a control arm. The screening arm participants were instructed to receive a chest radiograph and a sputum cytology test every four months for a period of six years. The control arm received an annual reminder in the mail to undergo a chest radiograph, in line with the 1970 Mayo recommendations, and also a follow-up survey. In addition to the six years of active trial, there was an additional year of follow-up.

Table 5.1 summarizes data on detected cancers found during the first seven years of the MLP trial, referenced by the enrollment date for each trial participant[18, 19]. A total of 151 lung cancers were detected in the screening arm whereas 120 lung cancers were detected in the control arm (an excess of 31 lung cancers in the screening arm). A higher percentage of the total number of lung cancers found in the screening arm was Stage I (79/151 or 53%) compared to the control arm (33/120 or 27.5%). A mortality review committee reviewed the causes of death for deceased participants during the trial. According to death certificate records, there were 82 deaths attributed to lung cancer in the screening arm (five were study-related deaths) and 70 lung cancer deaths in the control arm (an excess of 12 lung cancer and study-related deaths in the screening arm). In addition, there were 606 deaths by causes other than lung cancer

in the screening arm and 595 in the control arm.

In order to determine the impact of the MLP screening regimen on lung cancer mortality over a longer time frame, Marcus et al. (2000) searched death certificate records available through the National Death Index (NDI) reported on or before December 31, 1996. A detailed description of the search algorithm used to identify lung cancer deaths in trial participants is provided [40]. The search resulted in a total number of 337 lung cancer-attributed deaths in the screening arm versus 303 in the control arm (an excess of 34 deaths in the screening arm). In addition, there were 2,156 deaths by a cause other than lung cancer in the screening arm and 2,142 in the control arm. The median reported follow-up time was 20.5 years including the six-year trial duration. Table 5.2 summarizes the aggregated incidence and mortality data.

In addition, a further follow-up study identified additional lung cancer incidence cases in MLP participants through December 31, 1999 [Marcus06]. An assignment of lung cancer status relied upon data from multiple sources including medical records, next-of-kin and participant surveys, and death certificates. A detailed classification algorithm was used to assign a participant's lung cancer status and an assessment of the algorithm's validity and sensitivity was performed [41]. The search resulted in the identification of a total number of 585 lung cancers in the screening arm versus 500 in the control arm (an excess of 85 lung cancers in the screening arm). Due to the nature of the search methodology, 885 participants in the screening arm were classified as having an unknown lung cancer status, versus 943 in the control arm. Under the assumption that the ability to identify lung cancer status was independent of true lung cancer incidence, the authors projected a total of 724 lung cancer cases in the screening arm versus 630 in the control arm as of December 31, 1999 (an excess of 94 cancers in the screening arm). The median reported follow-up time was 23.5 years, including the six-year trial duration.

We obtained the original data recorded during the MLP trial and merged it with the patient-level records from the two long-term follow-up studies to form a unified MLP data-set. The original data collected during the MLP trial is made available to CISNET participants on its website. Data integrity is guaranteed by Phil Prorok, PhD of the National Cancer Institute (NCI). These data contain individual patient records on medical and smoking histories at the time of enrollment, annual follow-up questionnaire results, chest x-ray visit dates and findings, cytology results (including staging of lung diagnoses) as well as death records (including attributed causes of death by trial participants). Data from the two long-term follow-up studies was provided by Pamela Marcus, PhD, of the NCI. These data contain patient-level records on lung cancer incidence status as well as vital status and attributed causes of death during the respective follow-up periods.

1.4.2 Mayo CT

The Mayo CT study was a prospective cohort study which began in 1999 and recruited 1,520 individuals (788 male, 732 female), greater than 50 years of age, with a smoking history of more than 20 pack-years. The study was intended to assess the extent of a stage shift toward Stage IA and IB diagnoses among detected lung cancers resulting from screening by CT. Since the Mayo CT study was a single-arm study, no control arm exists. The absence of a control arm has prompted several modeling groups to simulate a control arm against which to compare the observed results [3].

All 1,520 participants received a baseline CT screen and also an annual CT scan for a period of four additional years. The study confirmed that in 68% of the patients (1,049), at least one non-calcified pulmonary nodule was identified. Up to six nodules were reported at each annual screen, including the prevalence screen, and each re-

ported nodule was followed separately over time. Recommendations regarding nodule follow-up were provided but decisions regarding patient management were left to the discretion of the attending physician. Confirmed cancers were classified as incidence, prevalence or interval/symptomatic cancers. Importantly, prevalence cancers are defined as those cancers that resulted from a visible nodule detected at the time of the prevalence screen, but possibly removed years later. Given this classification scheme and the high sensitivity of CT, the reported incidence cancers are likely to have arisen spontaneously during the period of screening.

A total of 66 cancers were found, comprised of 58 non-small cell lung cancers (NSCLC) and eight small cell lung cancers (SCLC). All cancers had available radiologic data with the exception of three interval cancers (2SCLC, 1 NSCLC). A summary of the Mayo CT findings for the 58 NSCLC is depicted in Table 5.10. There were equal numbers of prevalence and incidence cancers: 29 prevalence and 29 incidence cancers (including one interval cancer) in total. However, there were more than twice as many prevalence cancers in women than in men: 20 prevalence cancers in women and nine in men. There were 16 incidence cancers in men and 13 incidence cancers in women. However, in men, there were seven advanced-stage incidence cancers (one stage unknown) whereas in women, there were three advanced-stage incidence cancers. Among the 58 NSCLC cases, there were 13 NSCLC deaths reported in the data-base. Nine of the 13 total NSCLC deaths were attributable to males with reported incidence or interval NSCLC cases (Table 5.11).

We compare and contrast the maximum reported radiologic tumor diameter (mm) between incidence cancers detected in the Mayo Lung Project and the Mayo CT study. A summary of these findings can be found in Table 5.12. Among males in the Mayo CT, the median maximum reported radiologic tumor diameter was 7.96 mm (n=7) among Stage I cancers and 11.97 mm (n=7) among advanced-stage can-

cers. Among males in the Mayo Lung Project having measurable tumors, the median maximum reported radiologic tumor diameter was 24.00 mm (n=49) among Stage I cancers and 40.00 mm (n=30) among advanced-stage cancers. Therefore, for each data-set considered separately, early-stage cancers had a smaller tumor diameter than advanced-stage cancers, but advanced-stage cancers detected in the Mayo CT study were smaller than early-stage cancers detected in the Mayo Lung Project. We considered the possibility of contamination of Mayo Lung Project Stage I cancers with advanced-stage tumors. Due to a change in staging guidelines between the two studies, there were nine node-positive tumors among Stage I cancers in the Mayo Lung Project. However, after excluding the nine Stage I, node-positive cancers, the median maximum reported radiologic tumor diameter among Stage I cancers in the Mayo Lung Project decreased by 0.5 mm to 23.5 mm (n=40).

1.4.3 International Early Lung Cancer Action Program (I-ELCAP)

The International Early Lung Cancer Action Program (I-ELCAP) originated in New York and is now an international effort in lung cancer screening with 38 participating centers worldwide, under the direction of Claudia Henschke, MD, PhD of the Weill Cornell Medical College in New York. Each participating institution was permitted to set its own entry criteria but was required to adhere to the I-ELCAP screening protocol so that data can later be pooled. Enrollees in the trial must be at least 40 years old, and have elevated risk for lung cancer due to either a history of cigarette smoking or another type of environmental exposure. Each enrollee receives a baseline screen using low-dose CT. The workup of a positive result on the initial low-dose baseline CT and annual repeat screening differs. A key distinction between the baseline and annual repeat screenings is the size at which biopsy is performed by use of fine needle aspiration. For baseline screenings, nodules less than 15 mm in tumor di-

ameter are not biopsied in the absence of nodule growth (evaluated by a CT interval of 3 months). In contrast, for new nodules identified during annual repeat screening, biopsy is performed on nodules as small as 5 mm in the absence of further growth.

For 31,567 asymptomatic individuals, there were 410 lung cancers found to have lung cancer on the baseline screen, and there were 74 lung cancers that arose during annual repeat screens. Of the 410 baseline lung cancers, 348 were stage I (85%) and of the 74 annual repeat cancers, 64 were Stage I. Notably, the frequency of advanced-stage cancers is equal for baseline and annual repeat screenings. A comparison of radiologic tumor sizes directly prior to treatment for all annual-repeat cancers in the Mayo CT and I-ELCAP data-sets may be informative in explaining the decreased rate of advanced-stage annual repeat cancers in I-ELCAP. However, size data on I-ELCAP annual-repeat cancers is unavailable. We have obtained partial data for baseline cancers from the New York ELCAP with initial recorded radiologic sizes of the first-seen tumor nodule. A comparison of the first reported radiologic sizes of prevalence cancers between Mayo CT and ELCAP cancers is illustrated in Table 5.13.

1.4.4 Lung Screening Study (LSS)

The Lung Screening Study (LSS) was a pilot and feasibility study for the National Lung Screening Trial (NLST) designed to compare the use of chest x-ray versus low-dose computed tomography for lung cancer screening in over 50,000 high-risk individuals. The study began in September, 2000 and a total of 1660 subjects were randomized to the CT arm and 1658 randomized to the chest x-ray arm. The enrollment criteria restricted enrollment to individuals between the ages of 55 and 74 years old, with at least 30 pack-years of smoking. Former smokers were admitted if they met these criteria and quit within the last 10 years. As in the Mayo CT study, work-up of positive screens and individual patient management was left to the discretion

of the patients' personal health care provider.

Table 5.14 outlines the reported findings from the LSS study. A total of 40 lung cancers were reported in the CT arm and a total of 20 lung cancers were reported in the chest x-ray arm. Furthermore, there were a total of 16 Stage III-IV lung cancers detected in the CT arm and 9 Stage III-IV lung cancers detected in the chest x-ray arm. We note however that 9 of the stage III-IV lung cancers detected in the CT arm were detected at baseline. Due to small numbers of total cancers, the difference in advanced-stage cancers between the two groups was considered not statistically significant.

Chapter 2

Excess Lung Cancer Risk Estimation

2.1 Mathematical Models of Carcinogenesis

The process of carcinogenesis is known to consist of multiple stages. Mathematical models of this multi-stage process have been formulated and fitted to epidemiological data, offering a mechanistic explanation of age and exposure-related patterns of cancer incidence. According to the two-stage clonal expansion (TSCE) model, the process of carcinogenesis is governed by two rate-limiting stages [46]. A normal cell (NC) must first transform to become an intermediate cell (IC), an irreversible step called initiation. Next, an intermediate cell must give rise to a malignant cell (MC), which gives rise to cancer with certainty; this is known as transformation. The TSCE model parameterization also accounts for the clonal expansion of intermediate cells (promotion), a key model feature used to account for exposure effects such as smoking in carcinogenesis models of lung cancer [44]. Extensions of the TSCE model include a wide range of multi-stage stochastic models of carcinogenesis accounting for initiation, promotion, and progression [38, 47]. An earlier, distinct mathematical model of carcinogenesis by Armitage and Doll allows for several rate-limiting steps, but not

for clonal expansion of intermediate cells [1].

2.2 Atomic Bomb Survivor Data

Estimates of excess lung cancer risk attributable to radiation from medical imaging are largely based on models derived from data on Japanese atomic bomb survivors from Hiroshima and Nagasaki, collected as part of the extended Life Span Study (LSS). These estimates of excess lung cancer risk for a single time exposure, when extended to cumulative exposures of chest x-ray are approximately two orders of magnitude lower than needed to explain the lung cancer incidence trends in the MLP [8, 6]. Current estimates of chest x-ray lung organ dose range from 0.06 - 0.25 mSv [14, 26], whereas dose estimates reported at the time of the Mayo Lung Project were higher (approximately 0.7 mSv [16]). Estimates of excess lung cancer risk attributable to chest x-ray rely on linear scaling of estimated ERR/Sv [9]; if the true model is somewhat less than linear, then estimates of excess lung cancer risk based on these models will be higher. Moreover, the excess lung cancer risks derived from the LSS may be substantially underestimated with respect to the MLP cohort, due primarily to the MLP participants' older ages and therefore, longer smoking histories at the time of enrollment.

According to the TSCE model, if the pool of NC remains constant in adults and radiation acts only to transform normal cells to IC, the absolute excess lung cancer risk attributable to radiation exposure should not increase with age-at-exposure. Several analyses of the LSS data have found it to be consistent with a TSCE model parameterization that assumes radiation acts only to induce NC to become IC [34, 28] (initiation effect). An age-at-exposure effect on radiation-induced initiation rates is rejected despite evidence that birth cohort effects are significant in estimating the

parameters of the TSCE model [34]. A study using the Armitage-Doll model also supports the absence of an age-at-exposure effect on stage transition rates for most solid cancers [52]. An analysis that merges data on smoking history and radiation exposure suggests that the observed higher excess relative risk among older LSS individuals is a spurious finding that reflects differences in smoking histories by birth cohort and finds the joint effect of radiation exposure and smoking is consistent with an additive but not a multiplicative effect [53]. This latter result supports a model in which both radiation exposure and smoking act synchronously to increase the pool of IC (via initiation), but radiation does not act on the IC directly (via promotion or transformation).

The original publication of the LSS data reports that the excess lung cancer relative risk is nearly three times higher in individuals whose age-at-exposure is greater than 40 compared to individuals whose age-at-exposures are between 25 and 39 years and persists over time [62, 56]. As discussed, this finding has been attributed to birth cohort differences in smoking histories among LSS participants [53, 56]. However, a close inspection of the LSS data incorporating smoking histories indicates that this data subset is approximately half the original size with an age-at-exposure distribution shifted to the left due to the requirement that cohort members be alive at the time smoking histories were collected. The excess LC mortality risk observed in the MLP is restricted to the group of individuals over the age of 60 at the conclusion of the MLP, a group with virtually no representation in the combined smoking and LSS data-set [40, 53].

Other modeling studies have suggested that the LSS data is more consistent with a radiation effect on both promotion and initiation [27, 33] than with an initiation effect alone. Furthermore, due to a delay in data collection after the bombings: "second-hit" lung cancers arising during the earliest time window are necessarily absent from

the data-set. Additionally, several case-control studies examining the risk of second cancers following radiation treatment for a primary cancer do suggest a significant super-additive effect of smoking and radiation [20, 49, 21].

Theoretical considerations of the TSCE model may help reconcile the conflicting studies on excess lung cancer risk. If radiation acts on both rate-limiting stages, its observable effect on the second stage will be negligible in younger individuals due to the small number of IC [46]. As individuals age, the effect of radiation on the second stage will increase due to the growing population of IC. Smoking will tend to enhance this effect of age, due to its role in promotion and initiation. Consequently, the absence of an age-at-exposure effect and an observed additive relationship between smoking and radiation are expected as long as the accumulated number of IC is small. Current models derived from the LSS data assume that either excess lung cancer risk or excess lung cancer relative risk depend on gender and smoking history but not on age-at-exposure [8, 6], most consistent with a relatively young exposure group such as the LSS data subset from which they are derived [53].

The original TSCE model parameterization assumes that if an acute exposure acts on the second transition rate, then the excess risk will be evident after a short lag time following the exposure. A literal interpretation of the TSCE model is that IC comprise a homogeneous group of cells that have all accumulated a single mutation. The "second hit" occurs when the complementary gene is mutated, resulting in a loss of function phenotype. Our approach is tantamount to allowing the population of IC to be heterogeneous, while sharing a common growth advantage as well as an increased probability of acquiring a subsequent mutation. However, the number of mutations in any particular IC is random as are the number of total mutations needed to result in a cancer phenotype. It follows that an acute radiation exposure may act on an existing population of IC to either directly induce a second hit or to irreversibly

increase the probability of the second transition.

2.3 Mathematical Model of Natural Course of Lung Cancer

A mathematical model of the natural course of lung cancer in a screened population was previously described and calibrated to the initial seven years of MLP data [Fleehinger93]. This model accounts for the essential features of disease onset and progression which are: (1) the individual's lifetime susceptibility to lung cancer in a high-risk population of male smokers, (2) the distribution of the age of onset of lung cancer in susceptible high-risk male smokers, (3) the duration of early stage (Stage I) disease after lung cancer onset, (4) the duration of advanced stage (Stage II/III) disease, and (5) the distribution of the age of death by other causes. The following features of a screening regimen are superimposed onto the natural history model of disease to reconstruct the temporal trends observed in a screen-based detection program: (1) sensitivity of chest radiography to detect early stage disease, (2) sensitivity of chest radiography to detect late stage disease, (3) regimen adherence frequency among the screening arm participants, and (4) cure probability of detected early-stage disease. Table 5.3 provides a summary of the parameterization and distributional forms of the natural history and screening variables used in our analysis. The calibration and verification of the model fit is based upon the simulation of 2,500 sample trial populations. We compare the observed early stage incidence, advanced stage incidence, lung cancer deaths, and other-cause deaths in the first seven years of the MLP with the mean simulated values over the same time frame.

Two key modifications are made to the model of natural history of disease in order to refine the calibration and fit to the MLP data. In prior studies, the age at death by

other causes was assumed to have a trapezoidal distribution [15]. In our analysis, we use a table of smoking-history and age-dependent annual hazard rates to simulate the age at death by other causes than lung cancer. This hazard table was developed by Margie Rosenberg, PhD and provided as a CISNET resource (www.cisnet.cancer.gov). We verified the consistency of this hazard table with the MLP data; we estimate the age-specific hazards from the MLP trial directly and compare the associated cumulative distribution of age of death of other causes from both sources. In addition, we sample from the empirical distribution of age at enrollment of MLP participants in order to generate the age at enrollment in our simulations. This approach is in contrast to prior studies in which the distribution of the age at enrollment was assumed to be right-skew triangular [15].

We project lung cancer mortality and incidence in the follow-up period, extending the time frame of the simulation from seven to 24 years. We separately employ two different models of screening frequency in the follow-up period. The first model assumes that, upon completion of the MLP, the screen frequency of adherent screening arm participants reverts to baseline levels of random periodic screening. The second model assumes that, upon completion of the MLP, screening arm participants receive annual screening for a period of random duration, averaging ten years, after which they revert to baseline levels of random periodic screening.

2.4 Framework for Estimating Lung Cancer Risk in the MLP

We describe a biological framework for estimating excess lung cancer risk resulting from repeated chest Xray screens. As in the TSCE model, we assume two rate-limiting steps in the carcinogenesis process, namely the transition from NC to IC and

the transition from an IC to the first MC. Due to their smoking histories, we assume that by age 40, MLP participants have accumulated x_0 IC, which is an exponential random variable with parameter λ : $x_0 \sim \exp(\lambda)$. We assume a minimum number z of IC has accumulated in an individual by age 40, so that x_0 has a lower bound of z . Whereas the total number x_0 of IC at age 40 is stochastic, we assume that subsequently, the number of IC increases deterministically each year by a common factor c_i , where i represents indexing by attained age. The probability that a single IC becomes a MC in a given year is μ_s . Given an a priori set of discrete-time annual probabilities k_i of developing lung cancer at age i , we can express each k_i in terms of the parameters λ , μ_s , c_i , and z . As in the original natural course of lung cancer model, we assume that the age of lung cancer onset follows a right-skewed triangular distribution, such that $k_i = c(i - 39)$. We extend the range of age-of-onset from 80 to 85, while keeping the total lung cancer susceptibility equal to 0.226. This overall lower susceptibility compared to the simulation model reflects the fact that lung cancer cases that are treated and cured will not be represented in the mortality data.

In our model, radiation acts directly upon the IC to increase their genetic instability. For the periods during and prior to the MLP, we assume that the distribution of age of lung cancer onset is not influenced by radiation exposure due to screening. However, after the MLP has concluded, the probability that an IC becomes a MC increases to $\mu_s + k\mu_r$, for an individual having received k screens. Consistent with the assumption of deterministic growth of IC, the number of IC is assumed to be sufficiently large such that radiation exposure does not influence the total number of IC nor their annual growth rate. A depiction of the modified TSCE model is shown in Figure 1.

In the following section, we describe our methodology for estimating the key model parameters. To summarize, we first optimize the fit of the triangular lung cancer

age of onset distribution to the control arm data. This step entails updating the probability that a single IC transforms to an MC in a given year to $\mu'_s = \mu_s + \mu_{adj}$, and estimating the ratio $r_a = \frac{\mu_s + \mu_{adj}}{\mu_s}$ directly from the control group data. Next, we estimate the ratio $r_r = \frac{\mu'_s + \mu_r}{\mu'_s}$ from the screening arm data and evaluate whether r_r is significantly greater than one (equivalent to the case when μ_r is significantly greater than zero). Finally, we incorporate the estimate of r_r into a re-formulation of the discrete annual probabilities of lung cancer age of onset to derive the post-MLP annual age of lung cancer onset probabilities k'_i .

2.4.1 Mathematical Formulation of the Model

The annual probability of lung cancer onset at age i in the absence of radiation exposure, k_i , can be expressed as a function of the model parameters as follows:

$$k_i = \int_z^\infty (1 - \mu_s)^{\sum_{t=40}^{i-1} x_0 c_t} \lambda e^{-\lambda(x_0 - z)} dx_0, \text{ for } i = 40, \dots, 85.$$

Solving the integral in (1), we obtain:

$$k_i = \frac{-\lambda(1-\mu_s)^{\sum_{t=40}^{i-1} x_0 c_t}}{\ln(1-\mu_s)^{\sum_{t=40}^{i-1} x_0 c_t} - \lambda} + \frac{\lambda(1-\mu_s)^{\sum_{t=40}^i x_0 c_t}}{\ln(1-\mu_s)^{\sum_{t=40}^i x_0 c_t} - \lambda}, \text{ for } i = 40, \dots, 85.$$

Since $c_{40} = 1$, $c_i : i < 40 = 0$, $k_{40} = 1 + \frac{\lambda(1-\mu_s)^z}{\ln(1-\mu_s) - \lambda}$ and therefore: $\lambda = \frac{\mu_s(1-k_{40})}{e^{-\mu_s z} - (1-k_{40})}$.

It follows that $\sum_{t=40}^i k_t = 1 + \frac{\lambda(1-\mu_s)^z \sum_{t=40}^i c_t}{\ln(1-\mu_s)^{\sum_{t=40}^i c_t} - \lambda}$. Setting $x_i = (1 - \mu_s)^z \sum_{t=40}^i c_t$ and assigning a value to $\mu_s z$, we can apply Newton's method to solve for each x_i in the equation $\sum_{t=40}^i k_t - 1 = \frac{\lambda z x_i}{\ln x_i - \lambda z}$, and thereby obtain solutions for c_i . Provided that $e^{-\mu_s z}$ is sufficiently greater than $(1 - k_{40})$, the quantity $\mu_s z$ has little influence on the solutions for c_i . In this scenario, the probability that lung cancer onset will occur at age 40 in an individual with z intermediate cells, is negligible, and is consistent with maximal variance in the number of intermediate cells at age 40.

This mathematical framework allows for the modification of the discrete annual probabilities of lung cancer onset by incorporating changes in the probability that an IC transforms into a MC, relative to μ_s . For example, if the lifetime probability of IC transition increases from μ_s to $\mu_s + \mu_{adj}$, we let $r_{adj} = \frac{\mu_s + \mu_{adj}}{\mu_s}$, and after re-arranging (2), we obtain:

$$k'_i \approx \frac{-\lambda z(x_{i-1})_{adj}^r}{r_{adj} \ln(x_{i-1}) - \lambda z} + \frac{\lambda z(x_i)_{adj}^r}{r_{adj} \ln(x_i) - \lambda z}$$

However, our model assumes that excess lung cancer cases attributable to screening exposure are expected only after the MLP has concluded, resulting in a further modification of k'_i . We define $r_r = \frac{\mu'_s + \mu_r}{\mu'_s}$ and $r = \frac{\mu'_s + k\mu_r}{\mu'_s}$, where k is the number of screens received during the MLP, such that the relationship between r_{adj} , r_r , and r is defined by: $r = r_{adj}(1 + (r_r - 1)k)$. For a screening arm participant who received k screens and completed the MLP at age a , we define $r_{a,i} = \sum_{t=a+1}^i c_t / \sum_{t=40}^i c_t$, and expressed the annual probability of lung cancer after age a as follows:

$$k'_i \approx \frac{-\lambda z(x_a^{r_{adj}})(x_{i-1})^{rr(a,i-1)}}{r_{adj} \ln(x_a) + rr_{(a,i-1)} \ln(x_{i-1}) - \lambda z} + \frac{\lambda z(x_a^{r_{adj}})(x_i)^{rr(a,i)}}{r_{adj} \ln(x_a) + rr_{(a,i)} \ln(x_i) - \lambda z}$$

2.4.2 Likelihood-Based Estimation of the Model Parameters

In order to estimate the adjusted annual probabilities k'_i , reflecting the excess lung cancer risk attributable to screening, we first isolate the data from individuals who were alive at the end of the first seven years of the MLP trial and eligible for inclusion in the long-term follow-up analysis of lung cancer mortality. Outcomes are coded to reflect three possibilities: the participant was alive at the end of the follow-up period, he died of lung cancer, or he died of other causes. If a participant died of other causes, or was alive at the end of the follow-up period, then this record is censored

with respect to lung cancer onset. The number of screens each participant received during the first seven years of the MLP is also recorded. A summary of the relationship between screen frequency and subsequent lung cancer incidence and mortality is summarized in Tables 5.7 and 5.8.

Given a censoring event at age t , age at enrollment a_0 , we apply the Bayesian data-augmentation algorithm [63] to generate an age of lung cancer onset x from the distribution:

$$Pr[x = i | a_0, (s + x) \geq (a_0 + 7)] = \frac{k_i Pr[s > (t - i)] I_{\{a_0 \leq i < t\}} + k_i I_{\{i \geq t\}}}{1 - \sum_{j=40}^{a_0-1} k_j - \sum_{j=a_0}^{a_0+6} k_j Pr[s \leq (a_0 + 7 - j)]}$$

The time of lung cancer progression from lung cancer onset to death, s , has a distribution which is a convolution of two exponential distributions [15]. Using the augmented data, a likelihood function can be defined according to the following three scenarios:

Censored data, lung cancer onset at age i after data-augmentation:

$$Pr[x = i | a_0, (s + x) \geq (a_0 + 7)] = \frac{k_i Pr[s > (a_0 + 7 - i)] I_{\{a_0 \leq i < a_0 + 6\}} + k_i I_{\{i \geq a_0 + 7\}}}{1 - \sum_{j=40}^{a_0-1} k_j - \sum_{j=a_0}^{a_0+6} k_j Pr[s \leq (a_0 + 7 - j)]}$$

Censored data, no lung cancer onset after data augmentation:

$$Pr[x = \infty | a_0, (s + x) \geq (a_0 + 7)] = \frac{1 - \sum_{j=a_0}^{85} (k_j Pr[s > (a_0 + 7 - j)] I_{\{a_0 \leq j < a_0 + 6\}} + k_j I_{\{j \geq a_0 + 7\}})}{1 - \sum_{j=40}^{a_0-1} k_j - \sum_{j=a_0}^{a_0+6} k_j Pr[s \leq (a_0 + 7 - j)]}$$

Lung cancer death in original follow-up data-set at age t :

$$Pr[d = t | a_0, (s + x) \geq (a_0 + 7)] = \frac{\sum_{j=a_0}^t k_j Pr[(t - j) < s < (t - j + 1)]}{1 - \sum_{j=40}^{a_0-1} k_j - \sum_{j=a_0}^{a_0+6} k_j Pr[s \leq (a_0 + 7 - j)]}$$

We estimate r_{adj} using the Bayesian data augmentation as follows: 1) Augment con-

trol arm data n times with the initial condition: $r_{adj} = 1$. 2) Obtain the maximum likelihood estimate of r_{adj} (\hat{r}_{adj}) for each of n iterations. 3) Compute the mean value of \hat{r}_{adj} over the n iterations. 4) Repeat 1) with the mean of \hat{r}_{adj} from 3) until the mean value of \hat{r}_{adj} converges to the starting value.

To estimate r_r , we augment the study arm data n times with the initial conditions: $r_{adj} = \hat{r}_{adj}$, $r_r = 1$, allowing r_r only to vary in the estimation procedure. To test the significance of \hat{r}_r , at each iteration of 4) we compute the likelihood ratio, composed of the ratio of the likelihood with $r_{adj} = \hat{r}_{adj}$, $r_r = \hat{r}_r$ to the likelihood with $r_{adj} = \hat{r}_{adj}$, $r_r = 1$. According to statistical theory, twice the negative logarithm of the likelihood ratio has a chi-squared distribution with one degree of freedom. We validate the null distribution by bootstrapping the control arm data n times, applying data augmentation, and computing the p -value of the log likelihood ratio, under the chi-square assumption. A uniform distribution of p -values, under the null distribution, is expected and observed. If the median p -value in the augmented study arm sample (with convergence) is less than 0.05, then we conclude that \hat{r}_r is significant.

2.4.3 Simulations Using the Estimated Distribution of k'_i and Calculation of Lung Cancer Excess Risk

We incorporate the parameter r_r into the original k_i , assuming $r_{adj} = 1$ in order to rescale the mortality-derived estimates to fit an incidence distribution. We compute the 10-year excess lung cancer probability for an individual having received 5, 10, or 20 screens at the conclusion of the MLP, for attained ages of 50, 60, or 70. We also incorporate k'_i into our original simulation model and compare the simulation results to the observed follow-up data on incidence and mortality.

2.5 Results

2.5.1 Model Calibration and Stochastic Variability

Table 5.4 compares the simulated lung cancer incidence and deaths in the first seven years to the deaths and incidence observed in the MLP. Figure 2 illustrates the simulated mean annual incidence cases for both the stop-screen and ongoing-screen models and the simulated annual lung cancer deaths for the stop-screen model over the duration of the median follow-up period of mortality and incidence. The difference in the simulated mean annual lung cancer deaths between the stop-screen model and the ongoing-screen model is negligible and only the stop-screen model is shown. Table 5.5 summarizes these simulation results.

We evaluated the stochastic variability of our simulation results with respect to the observed cumulative lung cancer incidence and mortality differences (screening - control). Among the 2,500 individual trajectories in our simulations, we report the frequency of observing a difference in the cumulative lung cancer incidence greater than or equal to 85 cases after 23.5 years of follow-up. In the stop-screen model, there were 10 ($p=0.004$) such trajectories whereas in the ongoing-screen model, there were 26 ($p=0.0104$) such trajectories. We also report the frequency of observing a difference in the cumulative lung cancer deaths (screening - control) greater than or equal to 34 cases after 20.5 years of follow-up. In the stop-screen model, there were 132 ($p=0.0528$) such trajectories, and in the ongoing screen model, there were 106 ($p=0.0424$) such trajectories (Table 5.6).

2.5.2 Maximum Likelihood Estimation of Excess Risk

Beginning with the initial value of $r_{adj} = 0.925$ in the augmentation procedure, we obtain a median MLE of $r_{adj} = 0.925573$ and a mean MLE of 0.9261446 after 120 iterations, illustrating convergence of the estimate of r_{adj} . Next, we verify the assumed

null chi-square distribution. The distribution of p -values resulting from the likelihood ratio test after 30 iterations is approximately uniform with a median p -value of 0.437. Beginning with initial values $r_{adj} = 0.925$ and $r_r = 1.008$, we obtain a median MLE of $r_r = 1.00823$ and a mean MLE of $r_r = 1.0080$ after 125 iterations. The median p -value resulting from these 125 iterations is $p = 0.0021$.

Incorporating the parameter $r_r = 1.008$ ($p=0.0021$) into the original age-at-onset distribution, we estimate that the 10-year excess lung cancer probability for a 60-year old male smoker having received 10 chest X-ray screens is 0.574%. Figure 3 illustrates the 10-year probability of lung cancer at the conclusion of the MLP by attained age and the number of chest X-rays received.

2.5.3 Simulation of the Natural Course of Lung Cancer Assuming Excess Risk and Stochastic Variability

We repeat the MLP simulations after updating the annual probabilities of lung cancer onset k'_i with our obtained estimate of r_r . Within the spectrum of 1,000 individual trajectories in our simulations, we examined the frequency of observing a difference in the cumulative lung cancer incidence (screening - control) greater than or equal to 85 cases after 23.5 years of follow-up. In the stop-screen model there were 42 such trajectories ($p=0.042$). In the ongoing-screen model there were 53 ($p=0.053$) such trajectories. We also examined the frequency of observing a difference in the cumulative lung cancer deaths (screening - control) greater than or equal to 34 cases after 20.5 years of follow-up. In the stop-screen model there were 147 ($p=0.147$) such trajectories. In the ongoing-screen model, there were 115 ($p=0.115$) such trajectories.

2.6 Discussion and Conclusions

The usual interpretation of the MLP findings is that there is strong evidence that screening for lung cancer is plagued by over-diagnosis. In particular, there was no reduction in lung cancer mortality after the trial or after long-term follow-up [40] and the cumulative incidence of total lung cancer cases in the control arm did not "catch-up" to the cumulative incidence of total lung cancer cases found in the screening arm [41]. However, over-diagnosis does not explain the excess lung cancer deaths in the screening arm or the steady increase in lung cancer cases after the end of the MLP. At the end of 20.5 years of median follow-up, there were 34 more lung cancer-attributed deaths in the screening arm compared to the control arm. There were 31 more reported lung cancer cases in the screening arm versus the control arm at the end of the initial seven years of the MLP. At the end of 23.5 years of median follow-up, there were 85 more lung cancer cases detected in the screening arm compared to the control arm.

We examined the stochastic variability within our simulation model encompassing the time frame of the long-term incidence and mortality follow-up and discovered that the observed long-term incidence and mortality results deviate significantly from the expected mean behavior. A difference in the cumulative incidence of 85 or more cases after 23.5 years of follow-up occurred in only 0.40% and 1.04% of our simulation trajectories in the stop-screen and ongoing screen models, respectively. A difference in the cumulative number of lung cancer deaths of 34 cases or more after 20.5 years of follow-up occurred in only 4-5% of trajectories. While the observed data do lie within the range of variation that our model forecasts, their occurrence would be unlikely.

While our simulation model forecasts the total number of lung cancer deaths nearly exactly in the control arm, our model underestimates the number of lung cancer incidence cases by 53 cases in the control arm, excluding any projected cases among participants having unknown lung cancer status (Table 5.5). A key source of infor-

mation used to assign a participant's lung cancer status was based on next-of-kin questionnaire information [41]. The ability of next-of-kin to provide accurate information was determined by a sensitivity study based upon the ability of next-of-kin to correctly report lung cancer in already known lung cancer cases. Sensitivity was shown to be greater than 90%. However, a specificity study demonstrating the ability to correctly report the absence of lung cancer was not performed. Low specificity may have resulted in an inflation of reported lung cancer cases, thereby explaining the lack of consistency between reported lung cancer incidence and mortality in the follow-up period.

We sought a mechanistic explanation for the observed excess lung cancer risk among the screening arm participants. It has been suggested that the initial randomization procedures were flawed but this hypothesis has generally been discounted [41, 42]. The TSCE model predicts an age-at-exposure effect when the population of intermediate cells is large, such as expected in a population of high-risk smokers. The excess lung cancer mortality in the study arm participants was restricted to trial participants older than 55 at the time of enrollment and was greatest in individuals over the age of 65 at the time of enrollment. Furthermore, among screening arm participants, a higher number of screens received during the MLP trial corresponded to a higher frequency of lung cancer incidence and deaths reported in the follow-up period.

A Bayesian framework allows us to incorporate a single parameter of excess lung cancer risk, namely r_r , into an existing distribution of age-at-onset based on the triangular distribution. An advantage of our model-based estimation methodology is the improved power compared to traditional statistical methods for estimating excess risk. The parameter r_r was found to be highly significant ($p=0.0021$), due in part to the ability of our model framework to incorporate key correlates of excess lung cancer risk, age and screen frequency. The model-based predictions of 10-year excess lung

cancer probability recapitulate the observed relationship between excess lung cancer risk, attained age and screen frequency at the conclusion of the MLP.

Incorporating excess lung cancer risk into the simulation model of the natural course of lung cancer increases the likelihood of observing the differences in cumulative incidence and mortality (screening-control) as high as those observed in the reported long-term follow-up. We note two discontinuities between our estimation procedure and the simulation model. First, because we consider the number of screens to be a pre-existing factor in our estimation data-set, we eliminate any lung cancer deaths that occurred within the first seven years of the MLP, including the excess 12 lung cancer and study-related deaths in the study arm. Second, our simulation model of the MLP incorporates an estimate of early-stage disease curability of 35% and forecasts a net mortality benefit of six to seven deaths by year twelve. In our estimation procedure, the null hypothesis assumes equivalent lung cancer expected incidence and mortality in the screening and control arms following the conclusion of screening. This latter feature reflects the potentially conservative nature of our estimates of lung cancer excess risk.

In our view, the MLP results reiterate the value of the randomized trial in providing a measure of net mortality benefit, given uncertainty of the nature and quantification of the risks and benefits associated with early detection. In contrast to previous papers, our study suggests that excess lung cancer risk attributable to being a member of the screening arm of the MLP may provide a more satisfactory explanation of the MLP outcome than over-diagnosis. A reliance on an aggregate measure of trial efficacy to reflect one potential contributor of efficacy can be misleading. Our analysis further suggests the need for novel quantitative methods to directly estimate the stochasticity of tumor progression, and likewise, over-diagnosis.

As for the nature of the excess risk attributable to screening, a natural hypothesis invokes mutagenic effects of radiation. Our mathematical model has been formulated in such terms. However, other hypotheses might be invoked, such as a weakening of immunity by the stress of unknown nature caused by frequent screening. Since mutation rate results from a balance between DNA damage and repair, as well as removal of transformed cells, the net effects cannot be easily attributed to a single cause. Ideally, in the future, the risks associated with screening for lung cancer can be fully understood and successfully managed in order to maximize the number of lives saved by early detection.

Chapter 3

Tumor Progression Modeling

3.1 Introduction

A key component in the evaluation of the effectiveness of lung cancer screening strategies is the development of a descriptive model of lung cancer natural course. Once such natural history models are developed, screening strategies can be optimized with respect to variables such as the timing between screens, the clinical detection threshold upon which to act and treat early cancers. Ultimately, individual risk factors may be incorporated into the natural course model in order to personalize screening strategies. Key components of lung cancer natural course models include a characterization of population heterogeneity in tumor growth rates, the tumor size at which stage transition occurs, the correlation between tumor growth rate and size at stage transition as well as the relationship between cancer subtypes and these model variables. Despite the clear utility and value of lung cancer natural course models, they must be informed by data which are censored and incomplete. In a population of screened individuals, if a small, early lung cancer is detected, it is removed and the patient is treated. It is therefore unknown as to whether the cancer would progress and at what rate. Furthermore, cancer registry information provides a snapshot of advanced-stage symptomatic disease, typically of cancers arising in the absence of

screening. From registry data, the prior history of disease is unknown, in particular the duration of early-stage disease and the timing at which the stage transition occurred. In this chapter, we review data relevant to inference of models of lung cancer growth and progression and their current interpretation as well as underlying model parameter estimation strategies. We lay the foundation and background for a new statistical methodology used to evaluate data arising from different screening modalities, and thereby offering a more comprehensive view into the window of lung cancer natural course.

3.2 Relationship Between Tumor Size and Tumor Stage

The presence of a positive correlation between tumor size and tumor stage is a necessary but not sufficient condition supporting the basic premise of lung cancer screening, which is that small, early cancers detected by screening represent precursors to advanced-stage disease.

3.2.1 Cancer Registry Data

Evidence from the Surveillance, Epidemiology and End Results (SEER) cancer registry data supports the notion that the smaller the tumor size, the more likely it is that the cancer is in an early stage and has not yet spread to the lymph nodes or metastasized. In a study of 84,152 non-small cell lung cancer cases documented in the SEER cancer registry, among tumors less than 15 mm in diameter, the proportion of stage I cancers was 54% (N=7,327) whereas among tumors greater than 45 mm in diameter, the proportion of stage I cancers was 15% (N=31,623), with intermediate size strata reflecting a declining proportion of Stage I lung cancers [65]. The authors highlight that sampling biases in the SEER database, namely under-representation of small, asymptomatic early cancers and under-reported size information among large,

un-resected advanced stage cancers, are unlikely to negate the reported relationship between tumor size and stage, but rather to strengthen it [67, 65]. The presence of a stage shift among small T1 tumors (< 3 cm) is considered particularly relevant because active lung cancer screening has the ability to detect smaller lung cancers. In the SEER analysis, among tumors between 16 and 25 mm in diameter, 46% ($N=15,853$) were in Stage I, a significantly smaller percentage than the 54% proportion of Stage I cancers less than 15 mm in diameter [65]. We identified similar analyses of the stage distribution among T1 cancers stratified by size based on within-institution cancer registries. These studies had smaller sample sizes ($N < 1,000$) with correspondingly lower precision and in some cases failed to detect a stage shift [17, 31].

While sampling biases are known to affect statistical inferences based on cancer registry data, we furthermore note that cancer registry data are retrospective with respect to the natural course of lung cancer. Even if a stage shift with respect to size is shown to be present within a cancer registry, it does not preclude a scenario in which advanced-stage cancers undergo a stage transition at a small size and then proceed to grow rapidly until they reach the size at symptomatic detection. More compelling evidence would demonstrate a stage shift with respect to size prospectively, such as in a screening setting where all cancers are diagnosed at the smallest possible size threshold and there is a significant decline in the total number of advanced cancers relative to the number that are expected to arise in the absence of screening. We describe a new methodology for the prospective evaluation of cancers arising during screening in this chapter.

Also relevant to a model of lung cancer natural course are analyses of stage I lung cancers indicating that increasing tumor size is correlated with declining survival. If lung cancer progression is the result of genetic changes accumulated gradually over time, eventually leading to invasive and metastatic disease, then one might expect

that the larger the tumor, the more tumor cells present with the potential for causing a stage transition, and the worse the prognosis. We note however that an inverse relationship between tumor size and survival among stage I cancers may be circumstantially explained by higher rates of pseudo-disease among the smallest cancers. Extensive studies on the relationship between tumor size and survival within Stage I have been carried out with the aim of optimally defining the TNM staging criteria to include gradations of tumor size. A 1997 study based on data from MD Anderson Cancer Center found that among a group of 5,319 stage I cancers, there was a highly significant survival difference between two groups of Stage I cases separated by a size threshold of a 3 cm tumor diameter [48]. These data supported the introduction of revisions to the TNM staging criteria, namely to distinguish between Stage Ia and Stage Ib tumors [48] using a tumor size threshold of 3 cm. Many subsequent analyses of within-institution and SEER registries expanded the range of evidence used to support the TNM staging criteria and examine the 3 cm threshold [64, 43, 39, 51, 55, 10]. In particular, SEER data indicates that a 2 cm threshold distinguishing Stage Ia and Stage Ib tumors provides improved classification accuracy with respect to survival and that a further refinement of the size range among Stage Ib tumors ($> 3\text{cm}$) may be justified [43, 64]. These findings are incorporated in the recent revisions to the International Lung Cancer Staging guidelines in which the T component (tumor sizing) of the TNM methodology remains an important predictor of survival [13].

3.2.2 Lung Cancer Screening Data

Data from lung cancer screening trials differs significantly from cancer registry data. For one, active screening can lead to the detection of small, asymptomatic lung lesions. Studies based on chest radiography (x-ray) and more recent studies using CT clearly demonstrate the ability to detect increasingly small Stage I lung cancers with significant increases in five-year survival of screen-detected cancers. The Mayo Lung Project

has been described and the data outlined in Table 5.1. Within the initial seven-year period of active trial, the screening arm identified a total of 56 Stage I non-small cell lung cancers with a mean tumor diameter of 23.65 mm, and 48 advanced-stage non-small lung cancers with a mean tumor diameter of 41.07 mm (excludes 11 O/I cancers) whereas the control arm identified a total of 30 Stage I non-small cell lung cancers with a mean tumor diameter of 29.8 mm, and 55 advanced-stage non-small lung cancers with a mean tumor diameter of 47.14 mm (excludes 1 O/I cancer). Estimated five-year survival in the screening arm of the MLP was estimated to be as high as 70% for Stage I-detected cancers and as low as 10% for advanced-stage and interval cancers.

Computed tomography screening has demonstrated the ability to detect asymptomatic lesions at an increased rate compared to chest radiography, lower the size threshold for Stage I detection and increase further the estimated survival rates of screen-detected early-stage cancers. Data from the Mayo CT indicated that the size threshold for detection of early-stage cancers declined significantly to a mean tumor diameter of 9.42 mm for incidence cancers and 10.75 for prevalence cancers in males. Over 67% of enrollees in the Mayo CT were found to have at least one detected asymptomatic nodule. In the LSS study, the CT screening arm found 2.5 X as many Stage I cancers compared to the comparative chest x-ray arm. In the reported I-ELCAP study, 85% of all detected cancers were found to be Stage I, and the estimated survival was as high as 92% for Stage I-detected cancers that received surgical resection.

It is less clear whether the detection of Stage I cancers at a smaller size threshold corresponds to a decline in the frequency of detection of advanced stage cancers. For males in the Mayo CT, approximately 50% of non-small cell incidence cancers were advanced-stage cancers. In the LSS study, despite the increased number of Stage I cancers detected by CT, there were also nearly twice as many advanced-stage cancers

detected by CT compared to chest x-ray. A key concern is that while CT decreases the size threshold for the detection of early-stage cancers, it has also been shown to decrease the size threshold of detection of advanced-stage cancers. The mean tumor diameter of advanced-stage cancers in the Mayo CT was 14.76 mm among male incidence cancers, suggesting that the size threshold for curability of cancers with potential for stage transition may be low.

3.3 Lung Tumor Growth Rate and Over-diagnosis

Ultimately, natural history models are most useful when they accurately represent dynamic changes in tumor development. A key component of dynamic change is the rate of tumor growth over time. Given that the historical argument in favor of screening has been based on the relationship between tumor size and stage and corresponding survival improvements, the notion of over-diagnosis has taken on great importance. If small tumors detected by screening are very slow-growing, then the decrease in survival associated with increasing size is not relevant, because it will take a long time before small cancers exceed any given size threshold. In our view, of equal importance as the rate of over-diagnosis is the growth rate of advanced-stage cancers. In a worst case scenario, the bi-partite model suggests that all lung cancers are one of two types, either slow-growing, over-diagnosed cancers or else rapidly-growing aggressive cancers [2].

An accepted statistical methodology in the literature is to compare mortality rates between a screening and control arm and determine whether the difference in mortality is significant. The absence of a mortality reduction in the presence of a survival benefit for Stage I-detected cases has been attributed to over-diagnosis. We note however that other explanations are possible, including a systematic source of ex-

cess lung cancer risk attributable to screening (Chapter 2) or low power to detect a significant difference between screening and control arms. Other studies directly measure tumor growth rates and define the extent of over-diagnosis as the proportion of cancers with a doubling time greater than 400 days. Estimates of over-diagnosis have ranged from 5 to 50%. We note that direct studies of tumor growth have assumed an exponential growth model of lung cancer for which doubling times are constant. The assumption of constant tumor doubling times has more recently been challenged by more extensive longitudinal analyses of tumor growth [36]. Perhaps more importantly, traditional analyses of tumor growth introduce bias by excluding single-size measurements. Cancers arising due to single size measurements tend to be over-represented by larger prevalence cancers which are re-sected immediately and by incidence cancers that arise during annual-repeat screening, thereby biasing tumor growth measurements toward slower growth. An estimation methodology by Gorlova et al. (2005) incorporates both multiple and single-size measurements and estimates tumor growth from the Memorial Sloan Kettering Lung Screening Study [25].

3.4 Models of Lung Cancer Progression

In order to model the impact of screening in a population, a mathematical formulation of lung cancer natural course is needed. This natural history model assumes that cancer progresses in stages, beginning with an early, localized tumor, and progressing to advanced, metastatic disease. A simple model may account for the stochastic progression times of two stages (early and advanced) or it may account for tumor size (and growth), nodal involvement, and metastases (i.e. a random path through the TNM space). Walter and Day describe a statistical methodology for fitting a stochastic model in which the total progression time is represented by the convolution of two random variables and the duration of the early stage, or sojourn time, is

directly estimated [12]. A model using exponential duration of progression times has been described and fit to the Mayo Lung Project data. A key assumption is that all cancers arise from a common statistical distribution. We note however that this estimation methodology can potentially fit a wide range of observations resulting from a single randomized clinical trial, and may miss the underlying presence of bi-partite progression.

A model of size-driven progression may be represented by escalating hazard rates of stage transition with increasing size. Given an underlying growth model, the hazard rate of transition to a more advanced stage can be expressed by the following equation:

$$Pr[T \subseteq [t, t + \delta t) | T > t, S(t) = s] = h(s)\delta t + o(\delta t)$$

where T is the random age at which a stage transition occurs. $S(t)$ is the size at the stage transition and $h(s)$ is the size-dependent hazard rate of transition [5]. This assumption of size-dependent transition was adopted in the design of tumor progression models in breast cancer as well [54]. We note that the hazard rate of transition to a subsequent stage is typically assumed to be constant for a fixed size, independent of growth rate. Another important theoretical advance in modeling the relationship between tumor size and metastasis relates to the estimation of size-dependent transition probabilities [35]. Under the assumption that the detection probability is size-independent, the empirical distribution of tumor size at metastases can be used to estimate the probability of metastases at a given size. This methodology uses the fact that while tumor size at metastases is not observable, tumor size and metastatic spread at detection are and can be used to empirically reconstruct the former probability distribution.

3.5 Methods and Models

3.5.1 Simulation Analysis of Mayo CT Data

We first test how well our existing mathematical model of the natural course of lung cancer (Table 5.16) predicts the frequency of advanced-stage and early-stage cancers arising during the Mayo CT trial. In order to simulate the age at lung cancer onset in the Mayo CT trial, we use parameter estimates of the complete two-stage clonal expansion (TSCE) model derived by Meza et al. (2008) using data from the Nurses' Health and Health Professionals' Follow-up Studies [44]. This parameterization of the TSCE model incorporates Mayo CT participants' individual smoking histories as well as gender. We derive a hazard matrix for age at lung cancer onset using exact solutions to the hazard function of the TSCE model as given in Heidenreich (1997) [29], and condition each row of the matrix by participants' age at enrollment in the study. Furthermore, we increase the sensitivity of screen-detection in our model from 0.245 to 0.9 to reflect the increase in sensitivity of CT compared to chest x-ray. We note that our existing stochastic model of lung cancer progression models the stochastic duration of the early and advanced-stage of lung cancer but does not account for tumor growth or size-dependent stage transition. Therefore, this preliminary analysis is intended to examine whether the total numbers of early-stage and advanced-stage cancers identified in the Mayo CT study at baseline and during annual-repeat screening are consistent with the expected numbers of cancers and also to detect whether the increased sensitivity of CT results in a stage shift (reduction in advanced-stage cancers).

In order to examine the goodness of fit of the observed Mayo CT data to our simulation model, we simulate 2,500 iterations of the Mayo CT trial and compute the expected numbers of a) prevalence early-stage cancers b) prevalence advanced-stage cancers c) incidence early-stage cancers and d) advanced stage cancers for males, fe-

males, and both genders combined. Next, we compute a mean-squared error (MSE) statistic for males, females, and both genders combined based on the sum of squares of a) (total prevalence early-stage cancers - expected prevalence early-stage cancers) b) (total prevalence advanced-stage cancers - expected prevalence advanced-stage cancers) c) (total incidence early-stage cancers - expected incidence early-stage cancers) and d) (total incidence advanced-stage cancers - expected incidence advanced-stage cancers). For each of the simulated 2,500 iterations of the Mayo CT trial, we compute an MSE statistic in order to obtain a p -value reflecting the goodness of fit. We define the p -value as the proportion of simulated MSE values greater than or equal to the observed value.

We further define an adjusted MSE statistic in order to remove the effect of variation between the total expected and observed number of cancers. We compute a ratio r for males, females, and both genders combined, defined as $r = (\text{total expected cancers})/(\text{total observed cancers})$ and multiply it by the observed cancers in each grouping a), b), c) and d) as defined above. We re-compute the MSE statistic to reflect these adjusted values and compute the resulting p -value based on simulation of the MSE statistic as above, but with the incorporation of the ratio r for each iteration. Finally, we test the overall ability of an exponential model of duration of tumor progression to produce a suitable fit to the Mayo CT data. As a single-parameter distribution, the exponential model has the constraint that the mean and variance of the distribution be equal. We allow the original parameter estimates derived from the MLP to vary and evaluate the MSE statistic over a wide range of parameter combinations. We interpret these findings, in part, with respect to the constraints imposed on the shape of the exponential distribution.

3.5.2 Homogeneity Analysis of Mayo CT and Mayo Lung Project Data

Next, we examine the homogeneity between cancers arising during the MLP and the Mayo CT study with respect to the tumor size at stage transition. We assume an exponential model of tumor growth for which the exponential growth parameter is distributed according to the lognormal distribution. We incorporate estimates of log-normal tumor growth parameters for early and advanced cancers based on an examination of tumors arising during the Memorial Sloan Kettering study [25]. We assume that the size at stage transition x is governed by a Gaussian distribution $\Phi[x; \mu, \sigma]$, and is independent of tumor growth rate. Using this model, we estimate the mean size at stage transition for cancers in the Mayo Lung Project, the Mayo CT study, and for a combined data-set by maximum likelihood estimation. We test whether the maximum likelihood estimates (MLE) for the MLP and Mayo CT are significantly different by applying the likelihood ratio test having a chi-squared distribution with one degree of freedom. In order to derive a likelihood function for the mean size at stage transition μ , we summarize the data on tumor size and distribution of total counts for incidence cancers detected by screening as follows:

Table 3.1: Data Summary for Mayo CT and Mayo Lung Project data

	Early-Stage	Advanced-Stage
Mayo Lung Project	S_{11i}, n_{11i}	S_{12i}, n_{12i}
Mayo CT Study	S_{21i}, n_{21i}	S_{22i}, n_{22i}
Totals	$S_{.1i}, n_{.1i}$	$S_{.2i}, n_{.2i}$

For an early-stage cancer, we can express $Pr[x \geq S_{11i} | \mu] = 1 - \Phi[S_{11i} | \mu, \hat{\sigma}]$, estimating the variance in size at stage transition as the variance in observed sizes among observed early-stage cancers. For late-stage cancers, the likelihood function for the size at stage transition depends on the size at detection as well as the possible tumor

growth trajectories preceding cancer detection and the detection probability for early and advanced-stage cancers. We let m = the number of times an early cancer was missed on a prior screen, n = the number of times late cancer was missed, r_1 = the growth rate of the early-stage, and r_2 = the growth rate of the late-stage. Then, for a given combination of $(m, n, r_1, \text{ and } r_2)$, the size at stage transition x is confined to a fixed range defined by $f(m, n, r_1, r_2)$. We can express:

$$\begin{aligned} Pr[x \leq S_{12i} | \mu] &= \sum_{m, n, r_1, r_2} [\Phi(\max f(m, n, r_1, r_2) | \mu, \hat{\sigma}) \\ &- \Phi(\min f(m, n, r_1, r_2) | \mu, \hat{\sigma})] f(r_1) f(r_2) (1 - p_1)^m (1 - p_2)^n I_{\text{detection at } S_{12i}} \end{aligned}$$

Using these equations, we can formulate likelihoods and obtain the maximum likelihood estimates of μ_1, μ_2, μ_3 , the mean size at stage transition for the Mayo Lung Project, the Mayo CT, and the pooled group, respectively and determine whether the MLE estimates from the two data-sets are significantly different.

3.5.3 Data Visualization and Clustering of Mayo CT and Mayo Lung Project Data Based on Branching Fraction (f) and Cell Mutation Rate (μ)

We describe a new model used to represent the growth and size-driven transition for cancers in the Mayo Lung Project as well as the Mayo CT as a function of two evolutionary parameters, namely the stem cell branching fraction (f) and the cell mutation rate (μ). For each cancer, we simulate a likelihood function over the defined range of f and μ , which serves as a data visualization tool as well as a framework for clustering cancers into distinct categories reflecting growth rate and tumor aggressiveness. The model assumes that cancer arises from a single stem-like malignant progenitor cell. We assume that at the time of cell division, this progenitor cell gives rise to two iden-

tical stem-like cells with probability f and gives rise to one stem-like progenitor cell and one terminally differentiated cell with probability $1-f$. Tumor growth occurs as the result of the accumulation of cells from multiple cell divisions. We assume a pure-birth process in which terminally differentiated cells contribute to the overall size of the tumor but, unlike stem-like progenitor cells, do not undergo cell division events. We assume that the accumulation of n key mutations in a stem-like progenitor cell results in the development of an aggressive, advanced-stage tumor with invasive and metastatic properties. The probability of each of the n key mutations occurring at a cell division step is μ .

We collect data on tumor size, tumor stage, and the history of screens for incidence cancers arising during the MLP and Mayo CT studies. Since our model depends on the total cell count in the tumor, the assumption that the diameter of a single tumor cell is equal to $50 \mu m$ allows for conversion of tumor diameter to cell number based on the volume equation: $V = \frac{4}{3}\pi r^3$. We fix the range of parameter values for f and μ to be $f \in [0.0025, 0.0525]$ and $\mu \in [0.00001, 0.001]$. This range of parameter values encompasses the spectrum of doubling times reported in the literature and is consistent with estimates of a stem cell fraction of up to 5%. The mean size at stage transition over this parameter set ranges from 5 mm to 100 mm based on simulation studies (Table 5.15). In order to simulate the joint likelihood function of f and μ , we select a random value of f and μ from the joint uniform distribution and simulate the tumor trajectory. The decision to retain the sampled values of f and μ is contingent on the following conditions being satisfied:

- 1) For early-stage cancers, the simulated size at stage transition is larger than the size at detection
- 2) For advanced-stage cancers, the simulated size at stage transition is smaller than the size at detection
- 3) Given a screen history of prior screens, p , over the detectable range of tumor de-

tection and a random uniform variable $U \in [0, 1]$, with screen sensitivity s , we retain (f, μ) iff $U < (1 - s)^p$. For each cancer incidence case, replacement sampling is allowed to continue until 1,000 values of f and μ are generated. In order to perform sensitivity analysis with respect to the impact of the estimate for screen sensitivity s for chest x-ray detected cancers, we vary condition 3) to reflect a size-dependent model of screen detection. We assume that the probability of screen detection increases linearly with tumor diameter such that the probability of detection at a given screen equals $.1 + 0.12(\text{diam} - 5)$.

The simulated likelihoods are reserved for each tumor case separately. We fit a smoothed likelihood over a 10×10 grid using the Matlab `gridfit` function. For each data-set separately, we sum over the log likelihoods, obtain the maximum likelihood parameter estimates for the Mayo CT and MLP data-sets and perform a likelihood ratio test based on a chi-squared distribution with two degrees of freedom in order to test whether the MLP and Mayo CT data-sets are significantly different with respect to f and μ . We also consider the possibility that there are unique subsets of tumors governed by distinct combinations of the parameters f and μ . We construct a similarity matrix for the incidence cancers in the MLP data-set on the basis of likelihood similarity. For the n_1 incidence cancers in the MLP data-set, we construct an $n_1 \times n_1$ matrix reflecting the percent of overlap between all pair-wise comparisons of the likelihoods in which each likelihood is normalized to sum to one. The threshold for discordance for any given likelihood pair is set to be 10%. Clustering of MLP cancers allows for local optimization (minimizes total discordance) over the entire combinatorial space having 2^{n_1} elements. Clustering separates MLP cancers into three groups: Cluster A, Cluster B, and Cluster C. Cluster C is comprised of cancers that cannot be distinguished between Clusters A and B on the basis of likelihood dissimilarity. We cluster Mayo CT cancers similarly into three clusters and perform a likelihood ratio test based on a chi-squared distribution with two degrees of freedom for each

pair-wise comparison between the Mayo CT and MLP cluster sub-sets.

3.6 Results

3.6.1 Simulation Analysis of Mayo CT Data

A comparison of the mean numbers of simulated Mayo CT cancers with the actual trial findings are illustrated in Table 5.16. While the overall simulation predicted the total number of non-small cell lung cancers nearly exactly (57.5 simulated cancers versus 58 actual cases of NSCLC), the simulation model over-predicts the number of cancers in males (30.2 simulated cancers versus 25 actual cases of NSCLC), whereas it under-predicts the number of cancers in females (27.3 simulated cancers versus 33 actual cases of NSCLC). In males, an evaluation of the model fit with respect to the MSE statistic, gave a resulting un-adjusted p -value of $p = 0.042$, whereas the adjusted p -value was $p=0.022$. The largest contributor to the MSE statistic (48%) in males was the difference between simulated advanced-stage incidence cancers and (2 simulated) and the observed advanced-stage incidence cancers (9 observed). In females, an evaluation of the model fit with respect to the MSE statistic, gave a resulting un-adjusted p -value of $p = 0.284$, whereas the adjusted p -value = 0.386. The largest contributor to the MSE statistic (85%) in females was the difference between simulated early-stage incidence cancers (8.9 simulated) and the observed early-stage incidence cancers (14 observed). In the MSE evaluation of both genders combined, the un-adjusted p -value was $p = 0.126$ and the adjusted p -value was $p = 0.06$.

In order to test the ability of the exponential model to fit the Mayo CT data in males, we allowed the early-stage duration to range from two years to eight years and the advanced-stage duration to range from one year to five years. Over this parameter range, the minimum MSE statistic for the male Mayo CT data gave an un-adjusted

p -value of $p = 0.154$.

3.6.2 Homogeneity Analysis of Mayo CT and Mayo Lung Project Data

We generate the maximum likelihood estimate for the mean size at stage transition using the Mayo Lung Project and the Mayo CT study incidence data for males only. For the Mayo Lung Project, we estimate that the mean size at stage transition is 29.5 mm whereas in the Mayo CT, we estimate that the mean size at stage transition is 20.82 mm. In the pooled group, the estimated mean size at stage transition is 27.9 mm. Using the likelihood ratio test based on the chi-squared distribution with one degree of freedom, we obtain that the p -value is $p = 0.089$, suggesting that there is weak evidence that the data are not homogeneous with respect to the size-driven transition model.

3.6.3 Data Visualization and Clustering of Mayo CT and Mayo Lung Project Data Based on Branching Fraction (f) and Cell Mutation Rate (μ)

We simulate the likelihood distributions for 105 out of the 115 incidence non-small cell lung cancers in the MLP and for 15 out of 16 incidence non-small cell lung cancers in the Mayo CT, omitting cases that have non-measurable tumor sizes. After smoothing the likelihood function and combining the log likelihoods for each data-set individually, we obtain that the maximum likelihood estimates of f and μ in the MLP are $(f, \mu) = (0.04, 0.00015)$ for a size-independent model of screen detection and $(f, \mu) = (0.025, 0.00015)$ for a size-dependent model of screen detection, and in the Mayo CT data-set are $(f, \mu) = (0.04, 0.0045)$, a three-fold increase in the estimated cell mutation rate parameter μ . For the combined data-set, we estimate $(f, \mu) = (0.04, 0.0025)$ under the size-independent detection model for MLP cancers and

we estimate $(f,\mu)=(0.025,0.0025)$ under the size-dependent detection model for MLP cancers. After performing a likelihood ratio test on the data, we obtain that $p = 0.004$, $p = 0.0055$, respectively suggesting that a common parameter set does not define the two data-sets.

We cluster the MLP data-set on the basis of a concordance of 0.1 and achieve a loss function of zero, using a k-means clustering algorithm. For the size-independent model of detection, three clusters are obtained: Cluster A, Cluster B, and Cluster C. Cluster A contains 35 N0M0 cancers ranging in size from 16 mm to 70 mm. Cluster B contains 44 N1M0 or N1M1 cancers ranging in size from 14 mm to 80 mm and Cluster C contains 25 N0M0 cancers ranging in size from 5 mm to 15 mm and one N1M1 cancer of size 90 mm. We test whether the Mayo CT cancers are consistent with MLP clusters A, B, and C separately. The maximum likelihood estimates for Clusters A, B, and C respectively are $(f,\mu)=(0.04,0.00005)$, $(0.04,0.00075)$, and $(0.04,0.00015)$. When we compare these clusters with the Mayo CT cancers collectively and perform a likelihood ratio test on the data, as described above, we obtain that $p \leq 0.00001$, $p = 0.31957$, and $p = 0.01969284$, respectively suggesting that the 15 pooled Mayo CT incidence cancers are not inconsistent with the Cluster B N1M0/N1M1 cancers, but are inconsistent with the predominantly N0M0 cancers in Clusters A and C. Using a size-dependent model of detection, Cluster A, B, and C contain 34, 44, and 26 cases respectively. The maximum likelihood estimates for Clusters A, B, and C respectively are $(f,\mu)=(0.04,0.00005)$, $(0.04,0.00075)$, and $(0.04,0.00015)$. When we compare these clusters with the Mayo CT cancers collectively and perform a likelihood ratio test on the data, as described above, we obtain that $p \leq 0.00001$, $p = 0.3906$, and $p = 0.01438$.

3.7 Discussion

Our aim was to combine information on lung cancers detected prospectively by chest x-ray or CT, in order to obtain a more complete picture of lung cancer natural course. The combination of multiple data sources allows us to challenge the usual assumption that all cancers arising during screening derive from a single statistical model. We obtain the best fit to the combined data-sets when we isolate cancers into distinct clusters. We find that the cancers arising during the Mayo CT screening trial are consistent with the collection of aggressive cancers in the MLP, despite the smaller size of advanced Mayo CT cancers. In our view, these findings lend additional credibility to a bi-modal model of tumor progression, in which the subset of large early-stage cancers in the MLP may progress only slowly to advanced-stage disease and advanced-stage cancers, such as those detected in the Mayo CT undergo stage transition at a small size than expected. However, these results do not preclude the possibility of mortality reduction under a scenario of aggressive nodule management, rapid diagnosis and treatment.

We restrict our comparison in these analyses to lung cancers arising in male screen participants in the Mayo Lung Project and the Mayo CT study (approx. 50% female). Based on a simulation model calibrated to the MLP, the distribution of early-stage and advanced-stage cancers in the Mayo CT was un-expected ($p=0.022$). The model predicted a three-fold greater number of advanced-stage prevalence cancers compared to advanced-stage incidence cancers, whereas the reverse scenario was observed: 9 advanced-stage incidence cancers compared to one advanced-stage prevalence cancer. Furthermore, the model constraint of the exponential distribution of stochastic progression times appears to be challenged by this data-set suggesting that a distribution with greater density at both extremes is preferred. This scenario is consistent with a version of a bi-partite like model of tumor growth and progression.

A key finding is that advanced-stage cancers detected during the Mayo CT study were smaller than early-stage cancers detected during the Mayo Lung Project. An analysis based on the size at stage transition indicated that there was weak evidence that the mean size at stage transition was significantly smaller among Mayo CT cancers than Mayo Lung Project cancers. We interpret this result as indicating an overall lack of homogeneity between the two groups of incidence cancers given the model framework. A lack of homogeneity suggests a violation of the model assumption that tumor growth rate is independent of size at stage transition and likewise that distinct strata of tumor progression growth and progression have not been accounted for by the proposed model of growth and progression.

We construct a new model framework consistent with stem-cell driven tumor progression in which the accumulation of mutations in a subset of stem-like cells drives stage transition. The stochastic portion of the model is embedded in variable rates of stem-cell proliferation as well as variation in the rate of accumulation of mutations. This model framework has a data visualization component, given that the joint simulated likelihood for each detected cancer can be interpreted in terms of the model parameters f and μ . Similar to the homogeneity analysis described above, we find that the Mayo CT study and MLP cancers are not mutually consistent with a single parameter combination of f and μ . When we cluster the MLP cancers on the basis of likelihood concordance, we find that the Mayo CT study cancers are consistent with Cluster B, containing nearly all advanced-stage cancers in the MLP data-set, despite the larger size of the advanced-stage cancers in the MLP. These findings were robust against changes in the assumption of screen detection, in that a switch to a model of size-dependent screen detection did not alter the findings.

Given evidence of a stage shift in the Mayo CT study, one might expect screen-detected advanced-stage cancers to be small. In this scenario, screen-detected cancers

found in an advanced-stage will likely be smaller cancers that progressed before intervention could be implemented. However, absence of a stage shift *and* a small mean size of advanced-stage cancers suggests that the required clinical threshold for detection and curability is also quite small. The median size of advanced-stage cancers in the Mayo CT study was 11.97 mm, compared to 40.00 mm in the Mayo Lung Project.

We note that CT screening protocols implemented in different studies and different medical institutions differ with respect to nodule management and are not likely to have similar outcomes. The management of detected nodules in the Mayo CT was left to the discretion of the attending physician, as in the ongoing NLST trial. In contrast, the I-ELCAP protocol requires that fine needle aspiration be more aggressively and consistently employed as a diagnostic tool. Our analysis suggests that rapid diagnosis, appropriate classification of positive screen-detected nodules, and rapid treatment is expected to have a large effect on mortality reduction, if the threshold for clinical detection is set below 10 mm. In the I-ELCAP, despite the lack of a non-screened arm, there was an equal frequency (15%) of advanced-stage cancers among baseline cancers as among annual-repeat cancers, an improvement over the Mayo CT [30].

Given the ongoing National Lung Screening Trial (NLST) comparing chest xray to CT, we believe that model-based methodology and insights may prove to be particularly important, in addition to more established analysis methods of randomized clinical trial data.

Chapter 4

Summary and Future Directions

The overall theme of this thesis is the use of a model-based estimation framework in the analysis of clinical trial data in order to extract optimal information, generate insights and recommendations that may optimize clinical strategies in lung cancer screening. Based on this study, we can suggest two key ways in which lung cancer screening may be optimized. The first is by maximum dose reduction of lung cancer screening modalities. Using a model-based framework specific to excess risk of lung cancer in individuals with a prior smoking history, we find that there is a significant excess lung cancer risk associated with repeated screening by chest x-ray. While early detection by screening remains a promising means of lung cancer mortality reduction, it must be applied judiciously, given its potentially high risk. From the standpoint of a public health message, this study also re-iterates that lung cancer screening should not be viewed as a replacement for primary prevention by smoking cessation, given the risks. The second is optimal nodule management at a low clinical size threshold. Our analysis suggests that the size threshold for clinical detection and cure may be small. Key differences in trial protocol may therefore imply a large difference in mortality outcomes. In particular, the optimal use of diagnostic and treatment techniques such as fine needle aspiration, ablation, and other minimally invasive surgery is a key component of screening success. The evaluation of screening outcomes and screening

effectiveness should consider the entirety of the detection and treatment continuum.

Furthermore, if a low clinical threshold for detection is to be established, the improved ability to distinguish between aggressive and non-aggressive cancers is essential. If stem-like cells are responsible for driving tumor aggressiveness, then there may be a role for computational bioinformatic approaches and algorithms to identify cancers with large stem cell fractions, as an alternative to biomarker approaches in which a single protein marker is presumed to represent a uniform population of cells. Due to the proliferative capacity of stem-cells and the genetic instability of cancer, it will be interesting to examine tumor classification techniques dependent on the cellular-based mutation patterns present in diagnosed tumors. There is still much room for improvement in the classification of T1 tumors free of lymphatic spread or distant metastases.

Another extension of this research is the use of clinical trial data in lung cancer drug trials in order to test biological hypotheses. Whereas a dominant trend in statistical methodology of clinical trials has been to implement Bayesian methods in order to reduce the number of patients enrolled in a given clinical trial, such an approach ignores the potential of clinical trial data to test biological hypotheses. In this thesis, we show two examples of the value of model-based methods to give biological insights based on lung screening data. Other treatment models that incorporate patient response covariates may be optimally combined and considered in a model-based framework. In addition to genetic approaches, the use of additional and novel patient response variables is a way to incorporate patient heterogeneity into optimal treatment strategies, currently a limiting factor in progress against cancer, and lung cancer in particular. Model fitting is currently challenged by small data sizes and will be further challenged by additional efforts at data reduction. It will be of interest to explore further the statistical properties of model-fitting in a clinical trial setting as well as mining additional data-sets.

Chapter 5

Tables and Figures

Table 5.1: Total number of lung cancers found in screening and control subjects during the Mayo Lung Project (ending July 1, 1983) in the 7-year period after the initial screen.

Trial Arm	Mode of Detection	N	Stage I	Stage II	Stage III/IV
Screening Arm					
	Routine Xray	66	41	3	22
	Routine sputum	18	16	1	1
	Routine Xray and Sputum	6	4	1	1
	Interval Xray	22	13	2	7
	Interval Symptoms	37	5	0	32
	Interval death	2	0	0	2
	Total	151	79	7	65
Control Arm					
	Routine Xray	-	-	-	-
	Routine sputum	-	-	-	-
	Routine Xray and Sputum	-	-	-	-
	Interval Xray	34	24	1	9
	Interval Symptoms	86	10	1	75
	Total	120	34	2	84

Table 5.2: Lung cancer (LC) incidence and mortality and other-cause (OC) mortality in the seven-year period after the prevalence screen and after long-term follow-up in the Mayo Lung Project (median of 20.5 years for mortality data and 23.5 years for incidence data)

	Screening Arm	Control Arm	Difference (S-C)
Years 1-7			
LC Incidence	151	120	31
LC Deaths	82	70	12
OC Death	608	601	7
Post-Follow-up			
LC Incidence	585	500	85
LC Deaths	337	303	34
OC Death	2151	2139	12

Table 5.3: Summary of Distributions and Parameter Values Used in the Simulation of the Natural Course of Lung Cancer

Variable	Distribution	Parameters, NSCLC	Parameters, SCLC
Age at Enrollment	Empirical	N/A	N/A
Lifetime Susceptibility	Bernoulli	$p=0.174$	$p=0.0520$
Duration of Early Stage (years)	Exponential	Mean = 4	Mean = 1.75
Duration of Late Stage (years)	Exponential	Mean = 2	Mean = 1
Cure Probability	Bernoulli	$p=0.35$	$p=0$
Age at Onset	Left-Skew Triangular	Min=40, Max=80	Min=40, Max=80
Detection Probability	Bernoulli	$p=0.245$	$p=0.245$
Adherence to Screening Regimen	Bernoulli	$p=0.75$	$p=0.75$
Duration of Screen-Free Intervals (years) in Non-adherent group	Exponential	Mean = 2.2	Mean = 2.2

Table 5.4: Simulated Lung Cancer Incidence and Deaths Compared to MLP data in the 7-year period after the prevalence screen

Outcome Measure	Simulated	Mayo Lung Project
Screening Arm		
Stage I Incidence	70.7	79 (1)
Advanced-stage Incidence	71.4	72 (2)
Lung Cancer Deaths	71.2	82
Other-Cause Deaths	675.3	608 (1)
Control Arm		
Stage I Incidence	38.1	34
Advanced-stage Incidence	85.9	86
Lung Cancer Deaths	74.4	70
Other-Cause Deaths	675.7	601

Includes 16 sputum-detected cancers that were not visible by chest radiograph at the time of detection.

(2) Includes 2 sputum-detected cancers that were not visible by chest radiograph at the time of detection.

Table 5.5: Simulated Lung Cancer Incidence and Deaths Compared to Mayo Lung Project Follow-Up data

Outcome Measure	SS Model	OS Model	MLP
Screening Arm			
LC Incidence	453.6	460.5	585
LC Deaths	296.1	293.9	337
OC Deaths	2425.6	2425.9	2151
Control Arm			
LC Incidence	447.1	447.7	500
LC Deaths	302.4	302.8	303
OC Deaths	2421.1	2420.5	2139

Table 5.6: Measures of Variation in Cumulative Lung Cancer Incidence and Deaths Within 2,500 Simulated Trajectories Over the Median Follow-Up Period (Median of 20.5 Years for Mortality Data and 23.5 Years for Incidence Data)

Measure of Variation	SS Model	OS Model
Min. Incidence Diff. (S-C)	- 100	-95
Max. Incidence Diff. (S-C)	105	128
Number of Trajec. with Inc. Diff. ≥ 85	10 (p=0.004)	26 (p=0.0104)
Min. Diff. in LC Deaths	-96	-99
Max Diff. in LC Deaths	78	73
Number of Trajec. with Diff. in LC Deaths ≥ 34	132 (p=0.0528)	106 (p=0.0424)

Table 5.7: Lung Cancer Incidence During the Follow-up Period by the Number of Screens Received During the Mayo Lung Project (excludes participants who received a lung cancer diagnosis or died during the first seven years of the MLP and those who declined long-term follow-up)

	Trial Screens	No LC	LC	Unknown Status	% LC (Known)
Screening Arm					
	1-5	349	54	157	13.40%
	6-10	136	20	52	12.82%
	11-15	145	23	65	13.69%
	16-20	1875	328	603	14.89%
	21-29	33	9	8	21.43%
Total		2538	434	885	14.6%
Control Arm					
	1-5	2542	380	943	13.00%

Table 5.8: Lung Cancer Deaths During the Follow-up Period by the Number of Screens Received During the Mayo Lung Project (excludes participants who died during the first seven years of the MLP and those who were ineligible for long-term mortality follow-up)

	Trial Screens	Alive	OC Death	LC Death	% LC Death
Screening Arm					
	1-5	328	208	34	5.96%
	6-10	118	92	13	5.83%
	11-15	147	87	17	6.77%
	16-20	1500	1129	186	6.61%
	21-29	21	27	5	9.43%
Total		2114	1543	255	6.52%
Control Arm					
	1-5	2140	1538	233	5.96%

Table 5.9: Measures of Variation in Cumulative Lung Cancer Incidence and Mortality Within 1,000 Simulated Trajectories Over the Median Follow-Up Period (median of 20.5 years for mortality data and 23.5 years for incidence data). We incorporate the excess risk parameter r_r into a stop-screen (SS) model and an ongoing screen (OS) model

Measure of Variation	SS Model	OS Model
Mean. Incidence Diff. (S-C)	29.9	37.8
Number of Trajec. with Inc. Diff. ≥ 85	42 (p=0.042)	26 (p=0.053)
Mean. Diff. in LC Deaths	7.8	4.5
Number of Trajec. with Diff. in LC Deaths ≥ 34	147 (p=0.147)	115 (p=0.115)

Table 5.10: Summary of Mayo CT Incidence, Prevalence, and Interval Lung Cancer

Detection	Totals	Stage I	Stage II	Stage III/IV	Unknown	Small Cell
Males						
Prev.	9	8	1	0	0	1
Inc.	12	6	2	3	1	1
Inc-R.	3	1	1	1	0	0
Int.	1	0	0	0	1	0
Totals	25	15	4	4	2	2
Females						
Prev.	20	14	3	3	0	1
Inc.	9	7	1	1	0	3
Inc-R.	4	3	0	1	0	0
Int.	0	0	0	0	0	2
Totals	33	24	4	5	0	6
Both Genders						
Prev.	29	22	4	3	0	2
Inc.	21	13	3	4	1	4
Inc-R.	7	4	1	2	0	0
Int.	1	0	0	0	1	2
Totals	58	39	8	9	2	8

Table 5.11: Distribution of Lung Cancer Deaths among Mayo CT Participants

	Totals	Stage I	Stage II	Stage III/IV	Unknown	Small Cell
Males						
Prev.	1/9	0/8	1/1	0/0	0/0	1/1
Inc.	7/12	2/6	2/2	2/3	1/1	1/1
Inc-R.	1/3	0/1	1/1	0/1	0/0	0/0
Int.	1/1	0/0	0/0	0/0	1/1	0/0
Totals	10/25	2/15	4/4	2/4	2/2	2/2
Females						
Prev.	2/20	2/14	0/3	0/3	0/0	0/1
Inc.	0/9	0/7	0/1	0/1	0/0	1/3
Inc-R.	1/4	0/3	0/0	1/1	0/0	0/0
Int.	0/0	0/0	0/0	0/0	0/0	1/2
Totals	3/33	2/24	0/4	1/5	0/0	2/6
Both Genders						
Prev.	3/29	2/22	1/4	0/3	0/0	2/2
Inc.	7/21	2/13	2/3	2/4	1/1	2/4
Inc-R.	2/7	0/4	1/1	1/2	0/0	0/0
Int.	1/1	0/0	0/0	0/0	1/1	1/2
Totals	13/58	4/39	4/8	3/9	2/2	4/8

Table 5.12: Size Comparison of NSCLC Incidence Cancers in the Mayo Lung Project and the Mayo CT Study in males and females

		N	Median Diam. (mm)	Mean Diam. (mm)
MLP				
	Males			
	Stage I	49/56	24.00	23.65
	Stage II/III	30/48	40.00	41.07
Mayo CT				
	Males			
	Stage I	7	7.96	9.42
	Stage II/III	7	11.97	14.76
	Unknown	2	11.43	11.43
	Females			
	Stage I	10	8.00	9.56
	Stage II/III	3	14.00	17.75

Table 5.13: Size Comparison of NSCLC Prevalence Cancers in the Mayo Lung Project, Mayo CT, And ELCAP Studies in males and females

		N	Median Diam. (mm)	Mean Diam. (mm)
MLP				
	Males			
	Stage I	25/28	22.00	31.44
	Stage II/III	29/39	55.00	54.76
Mayo CT				
	Males			
	Stage I	8	9.21	10.75
	Stage II/III	1	15.00	15.00
	Females			
	Stage I	14	8.62	9.44
	Stage II/III	6	12.99	19.23
ELCAP				
	Males			
	Stage I	21	10.88	13.24
	Stage II/III	2	23.75	23.75
	Females			
	Stage I	47	12.00	13.13
	Stage II/III	7	12.00	13.43

Table 5.14: Total Lung Cancer Cases in the Lung Screening Study in Baseline and Year 1

	CT Arm	Chest Xray Arm
Baseline		
Stage I	16	6
Stage II	3	0
Stage III	6	0
Stage IV	3	0
Unknown	2	1
Totals	30	7
Year 1		
Stage I	2	2
Stage II	0	1
Stage III	5	4
Stage IV	1	1
Unknown	0	1
Totals	8	9
Interval		
Stage I	1	0
Stage II	0	0
Stage III	0	1
Stage IV	1	3
Unknown	0	0
Totals	2	4

Table 5.15: Expected Size at Stage Transition as a Function of Parameters f and u

Log (Mutation Rate (u))	Branching Fraction						
	0.0025	0.005	0.01	0.02	0.03	0.04	0.05
-5.0	84.43	96.4	100	100	100	100	100
-4.5	34.0	65.1	80.4	100	100	100	100
-4.0	7.9	12.6	20.5	37.3	42.3	62.1	66.1
-3.5	5	5.5	7.2	10.6	13.9	14.0	22.1
-3.0	5	5	5	5	5	5	6.3

Table 5.16: Simulation of Mayo CT Incidence, Prevalence, Non-Small Cell Lung Cancers by Stage and Detection

	Sim, Sens. = 0.9	Sim, Sens. = 0.8	Actual
Males			
Prev, Early-Stage.	10.5	10.1	8
Prev, Adv.-Stage	6.3	6.5	1
Inc, Early-Stage	11.5	10.9	7
Inc, Adv.-Stage	1.9	2.1	9
Totals	30.2	29.6	25
Females			
Prev, Early-Stage.	8.9	8.7	14
Prev, Adv.-Stage	5.1	5.2	6
Inc, Early-Stage	11.5	11.2	10
Inc, Adv.-Stage	1.8	2.2	3
Totals	27.3	27.3	33
Both Genders			
Prev, Early-Stage.	19.4	18.8	22
Prev, Adv.-Stage	11.4	11.7	7
Inc, Early-Stage	23	22.1	17
Inc, Adv.-Stage	3.7	4.3	12
Totals	57.5	56.9	58

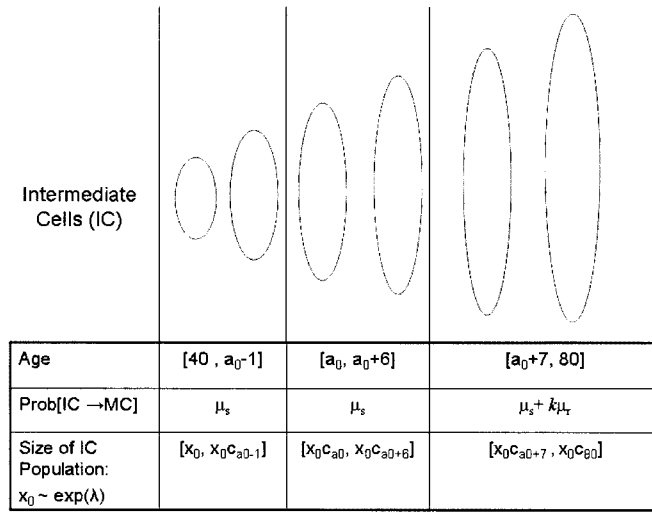
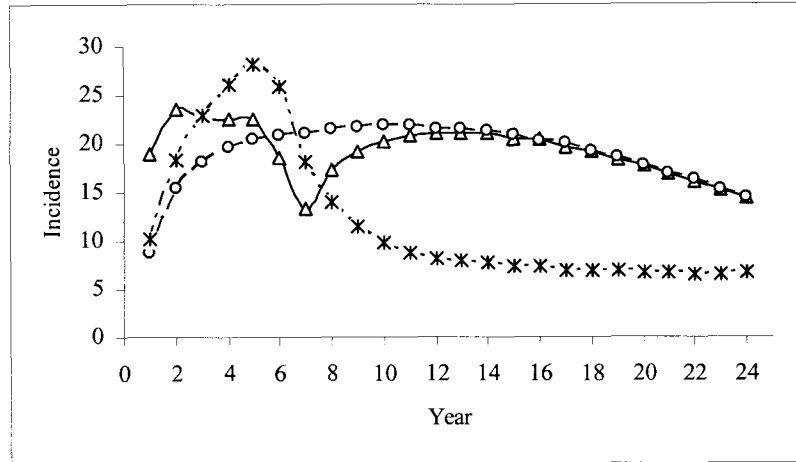
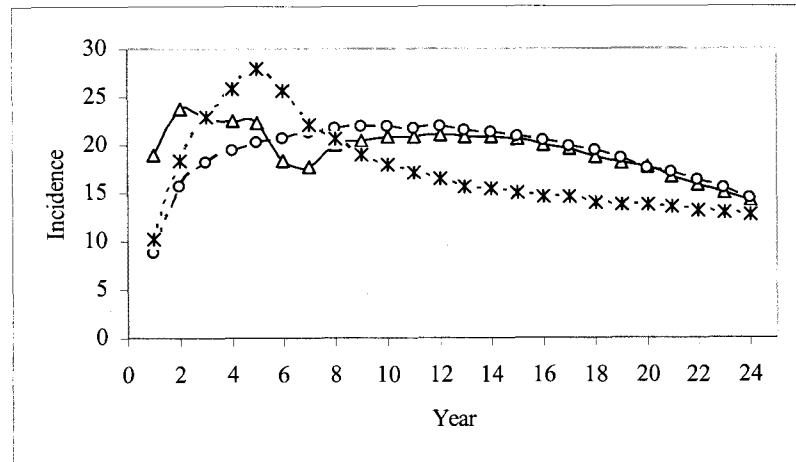


Figure 1. Depiction of the modified TSCE expansion model

a)



b)



c)

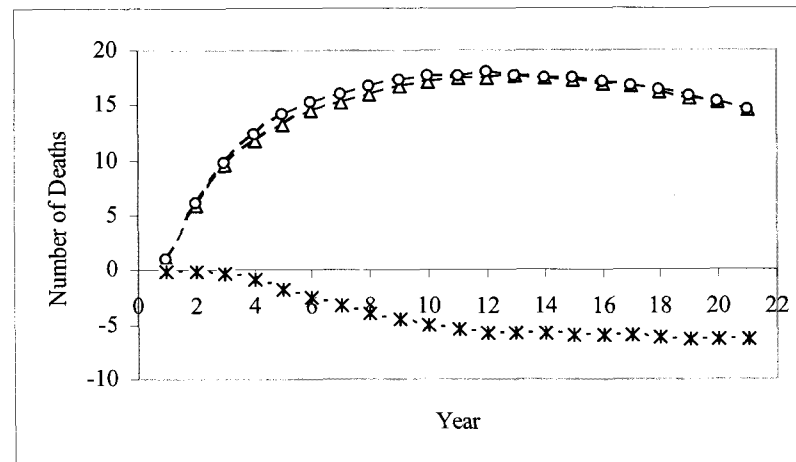


Figure 2. Simulated annual incidence, annual mortality and cumulative differences in incidence and mortality (screening-control) over long-term follow-up: a) Mean counts of lung cancer cases

per year assuming a stop-screen model. b) Mean counts of lung cancer cases per year assuming an ongoing screening model c) Mean counts of lung cancer deaths per year assuming a stop-screen model. Screening arm (Δ), control arm (\circ) and cumulative difference (*).

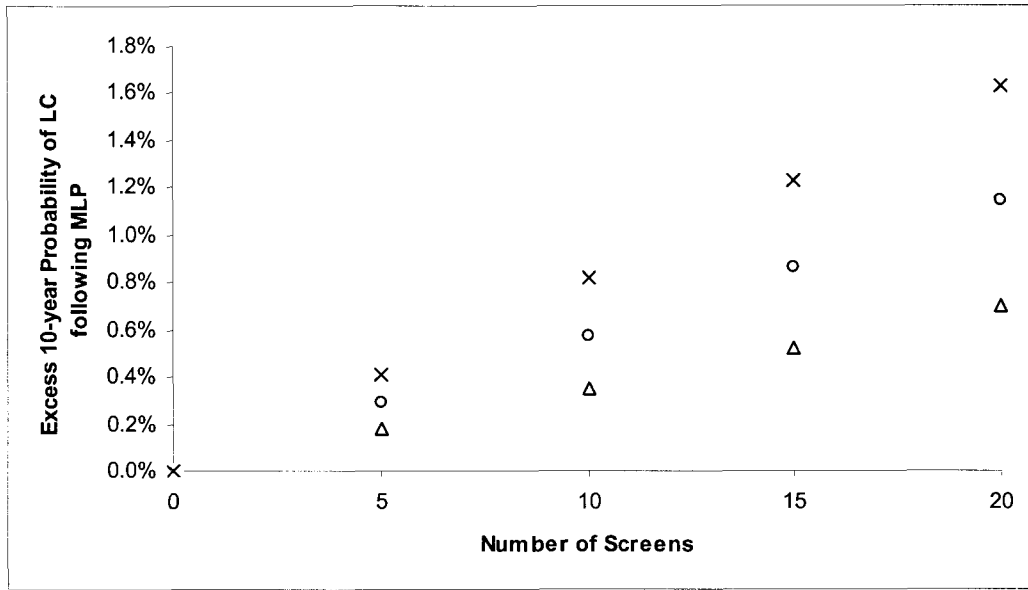


Figure 3. Model-predicted excess 10-year probability of lung cancer at the conclusion of the MLP by attained age and the number of chest Xrays received. 50 years-old (Δ) 60 years-old (\circ) and 70 years-old (\times).

Bibliography

- [1] P. Armitage and R. Doll. A two-stage theory of carcinogenesis in relation to the age distribution of human cancer. *British Journal of Cancer*, 11:161–69, 1957.
- [2] P.B. Bach. Is our natural history model of lung cancer wrong? *Lancet Oncology*, 9:693–697, 2008.
- [3] P.B. Bach, J.R. Jett, U. Pastorino, M.S. Tockman, S.J. Swensen, and C. Begg. Computed tomography screening and lung cancer outcomes. *JAMA*, 297(9):953–961, 2007.
- [4] P.B. Bach, G.A. Silvestri, M. Hanger, and J.R. Jett. Screening for lung cancer: Accp evidence-based clinical practice guidelines (2nd edition). *Chest*, 132(3):69S–77S, 2007.
- [5] R. Bartoszynski, L. Edler, L. Hanin, A. Kopp-Schneider, L. Pavlova, A. Tsodikov, A. Zorin, and A. Yakovlev. Modeling cancer detection: tumor size as a source of information on unobservable stages of carcinogenesis. *Mathematical Biosciences*, 171:113–142, 2001.
- [6] A. Berrington de Gonzalez and S. Darby. Risk of cancer from diagnostic x-rays: Estimates for the uk and 14 other countries. *The Lancet*, 363:345–351, 2004.
- [7] W.C. Black. Overdiagnosis: An underrecognized cause of confusion and harm in cancer screening. *Journal of the National Cancer Institute*, 92(16):1280–1282, 2000.

- [8] D.J. Brenner. Radiation risks potentially associated with low-dose ct screening of adult smokers for lung cancer. *Radiology*, 231:440–445, 2004.
- [9] D.J. Brenner and R.K. Sachs. Estimating radiation-induced cancer risks at very low doses: rationale for using a linear no-threshold approach. *Radiation and Environmental Biophysics*, 44:253–56, 2006.
- [10] Y.B. Chao, J.R. Masterman, M.S. Huberman, S.P. Gangadharan, D.C. McDonald, M.S. Kent, and M.M. DeCamp. Subdivision of the t1 size descriptor for stage i non-small cell lung cancer has prognostic value: A single institution experience.
- [11] T.V. Colby, H.D. Talezaar, W.D. Travis, E.J. Bergstralh, and J.R. Jett. A pathologic review of the mayo lung project. *Cancer*, 95(11):2361–2365, 2002.
- [12] N.E. Day and S.D. Walter. Simplified models of screening for chronic disease: estimation procedures from mass screening programmes. *Biometrics*, 40:1–14, 1984.
- [13] F.C. Detterbeck, D.J. Boffa, and L.T. Tanoue. The new lung cancer staging system.
- [14] S. Diederich and H. Lenzen. Radiation exposure associated with imaging of the chest: comparison of different radiographic and computed tomography techniques. *Cancer Supplement*, 89:2457–60, 2000.
- [15] B.J. Flehinger, M. Kimmel, T. Polyak, and M.R. Melamed. Screening for lung cancer: The mayo lung project revisited. *Cancer*, 72:1573–1580, 1993.
- [16] B.J. Flehinger, M.R. Melamed, R.T. Heelan, C.M. McGinnis, M.B. Zaman, and N. Martini. Accuracy of chest film screening by technologists in the new york early lung cancer detection program. *American Journal of Roentgenology*, 131:593–97, 1978.

- [17] D.B. Flieder, J.L. Port, R.J. Korst, P.J. Christos, M.A. Levin, D.E. Becker, and N.K. Altorki. Tumor size is a determinant of stage distribution in t1 non-small cell lung cancer.
- [18] R.S. Fontana, D.R. Sanderson, W.F. Taylor, L.B. Woolner, W.E. Miller, J.R. Muhm, and M.A. Uhlenhopp. Early lung cancer detection: Results of the initial (prevalence) radiologic and cytologic screening in the mayo clinic study. *American Review of Respiratory Disease*, 130:561–565, 1984.
- [19] R.S. Fontana, D.R. Sanderson, L.B. Woolner, W.F. Taylor, E. Miller, and J.R. Muhm. Lung cancer screening: The mayo program. *Journal of Occupational Medicine*, 28(8):746–750, 1986.
- [20] M.B. Ford, A.J. Sigurdson, E.S. Petrusis, C.S. Ng, B. Kemp, C. Cooksley, M. McNeese, B.J. Selwyn, M.R. Spitz, and M.L. Bondy. Effect of smoking and radiotherapy on lung carcinoma in breast cancer survivors. *Cancer*, 98(7):1457–1464, 2003.
- [21] E.S. Gilbert, M. Stovall, M. Gospodarowicz, F.E. van Leeuwen, M. Andersson, B. Glimelius, T. Joensuu, C.F. Lynch, R.E. Curtis, E. Holowaty, H. Storm, E. Pukkala, M.B. van't Veer, J.F. Fraumeni Jr., J.D. Boice Jr., E.A. Clarke, and L.B. Travis. Lung cancer after treatment for hodgkin's disease: Focus on radiation effects. *Radiation Research*, 159:161–173, 2003.
- [22] J.K. Gohagan, P.M. Marcus, R.M. Fagerstrom, P.F. Pinsky, B.S. Kramer, and P.C. Prorok. Baseline findings of a randomized feasibility trial of lung cancer screening with spiral ct scan versus chest radiograph: The lung screening study of the national cancer institute.
- [23] J.K. Gohagan, P.M. Marcus, R.M. Fagerstrom, P.F. Pinsky, B.S. Kramer, P.C. Prorok, S. Ascher, W. Bailey, B. Brewer, T. Church, D. Engelhard, M. Ford, M. Fouad, M. Freedman, E. Gelmann, D. Gierada, W. Hocking, S. Inampudi,

- B. Irons, C.C. Johnson, A. Jones, P. Kucera, G. Kvale, M. Oken, M. Plunkett, H. Price, D. Reding, T. Riley, M. Schwartz, D. Spizarny, R. Yoffie, and C. Zylak. Final results of the lung screening study, a randomized feasibility study of spiral ct versus chest x-ray screening for lung cancer.
- [24] O.Y. Gorlova, M. Kimmel, and C. Henschke. Modeling of long-term screening for lung carcinoma. *Cancer*, 92:1531–40, 2001.
- [25] O.Y. Gorlova, B. Peng, D. Yankelevitz, C. Henschke, and M. Kimmel. Estimating the growth rates of primary lung tumours from samples with missing measurements. *Statistics in Medicine*, 24:1117–1134, 2005.
- [26] E.J. Hall and D.J. Brenner. Cancer risks from diagnostic radiology. *British Journal of Radiology*, 81:362–378, 2008.
- [27] W.F. Heidenreich, H.M. Cullings, S. Funamoto, and H.G. Paretzke. Promoting action of radiation in the atomic bomb survivor carcinogenesis data? *Radiation Research*, 168:750–756, 2007.
- [28] W.F. Heidenreich, P. Jacob, and H.G. Paretzke. Exact solutions of the clonal expansion model and their application to the incidence of solid tumors of atomic bomb survivors. *Radiation Environmental Biophysics*, 36:45–58, 1997.
- [29] W.F. Heidenreich, E.G. Luebeck, and S.H. Moolgavkar. Some properties of the hazard function of the two-mutation clonal expansion model. *Risk Analysis*, 17(3):391–399, 1997.
- [30] C.I. Henschke, D.F. Yankelevitz, D.M. Libby, M.W. Pasmantier, J.P. Smith, O.S. Miettinen, and International I-ELCAP Investigators. Survival of patients with stage i lung cancer detected on ct screening. *New England Journal of Medicine*, 355(17):1763–1771, 2006.

- [31] L.E. Heyneman, J.E. Herndon, P.C. Goodman, and E.F. Patz Jr. Stage distribution in patients with a small (≤ 3 cm) primary non-small cell lung carcinoma: Implication for lung carcinoma screening.
- [32] L.L. Humphrey, S. Teutsch, and M.S. Johnson. Lung cancer screening with sputum cytologic examination, chest radiography, and computed tomography: An update for the u.s. preventive services task force. *Annals of Internal Medicine*, 140:740–753, 2004.
- [33] V. Jacob and P. Jacob. Modelling of carcinogenesis and low-dose hypersensitivity. an application to lung cancer incidence among atomic bomb survivors. *Radiation Environmental Biophysics*, 42:265–273, 2004.
- [34] M. Kai, E.G. Luebeck, and S.H. Moolgavkar. Analysis of the incidence of solid cancer among atomic bomb survivors using a two-stage model of carcinogenesis. *Radiation Research*, 148:348–358, 1997.
- [35] M. Kimmel and B.J. Flehinger. Non-parametric estimation of the size-metastasis relationship in solid cancers. *Biometrics*, 47:987–1004, 1991.
- [36] R.M. Lindell, T.E. Hartman, S.J. Swensen, J.R. Jett, D.E. Midthun, and J.N. Mandrekar. Five-year cancer screening experience, growth curves of 18 lung cancers compared to histologic type, ct attenuation, stage, survival, and size. *Chest*, 2009.
- [37] R.M. Lindell, T.E. Hartman, S.J. Swensen, J.R. Jett, D.E. Midthun, H.D. Tazeelaar, and J.N. Mandrekar. Five-year lung cancer screening experience: Ct appearance, growth rate, location, and histologic features of 61 lung cancers. *Radiology*, 242(2):555–562, 2007.
- [38] M.P. Little, W.F. Heidenreich, S.H. Moolgavkar, H. Schollnberger, and D.C. Thomas. Systems biological and mechanistic modelling of radiation-induced cancer. *Radiation and Environmental Biophysics*, 47:39–47, 2008.

- [39] A. Lopez-Encuentra, J.L. Duque-Medina, R. Rami-Porta, A. Gomex de la Cámara, and P. Ferrando. Staging in lung cancer: Is 3 cm a prognostic threshold in pathologic stage i non-small cell lung cancer?: A multicenter study of 1,020 patients.
- [40] P.M. Marcus, E.J. Bergstralh, R.M. Fagerstrom, D.E. Williams, R.S. Fontana, W.F. Taylor, and P.C. Prorok. Lung cancer mortality in the mayo lung project: Impact of extended follow-up. *Journal of the National Cancer Institute*, 92(16):1308–1316, 2000.
- [41] P.M. Marcus, E.J. Bergstralh, M.H. Zweig, A. Harris, K.P. Offord, and R.S. Fontana. Extended lung cancer incidence follow-up in the mayo lung project and overdiagnosis. *Journal of the National Cancer Institute*, 98(11):748–756, 2006.
- [42] P.M. Marcus and P.C. Prorok. Re-analysis of the mayo lung project data: the impact of confounding and effect modification. *Journal of Medical Screening*, 6:47–49, 1999.
- [43] C.M. Mery, A.N. Pappas, B.M. Burt, R. Bueno, P.A. Linden, D.J. Sugarbaker, and M.T. Jaklitsch. Diameter of non-small cell lung cancer correlates with long-term survival.
- [44] R. Meza, W. Hazelton, G.A. Colditz, and S.H. Moolgavkar. Analysis of lung cancer incidence in the nurses' health and the health professionals' follow-up studies using a multistage carcinogenesis model. *Cancer Causes Control*, 19:317–328, 2008.
- [45] O.S. Miettinen. Screening for lung cancer: Do we need randomized trials? *Cancer Supplement*, 89(11):2449–2452, 2000.
- [46] S.H. Moolgavkar and A.G. Knudson. Mutation and cancer: A model for human carcinogenesis. *Journal of the National Cancer Institute*, 66(6):1037–1052, 1981.

- [47] S.H. Moolgavkar and E.G. Luebeck. Multistage carcinogenesis and the incidence of human cancer. *Genes, chromosomes, and cancer*, 38:302–06, 2003.
- [48] C.F. Mountain. Revisions in the international system for staging lung cancer.
- [49] A.I. Neugut, T. Murray, J. Santos, H. Amols, M.K. Hayes, J.T. Flannery, and E. Robinson. Increased risk of lung cancer after breast cancer radiation therapy in cigarette smokers. *Cancer*, 73(6):1615–1620, 1994.
- [50] E.F. Patz. Lung cancer screening, overdiagnosis bias, and re-evaluation of the mayo lung project. *Journal of the National Cancer Institute*, 98(11):724–725, 2006.
- [51] E.F. Patz Jr., S. Rossi, D.H. Harpole, J.E. Herndon, and P.C. Goodman. Correlation of tumor size and survival in patients with stage ia non-small cell lung cancer.
- [52] D.A. Pierce and M.L. Mendelsohn. A model for radiation-related cancer suggested by atomic bomb survivor data. *Radiation Research*, 152:642–654, 1999.
- [53] D.A. Pierce, G.B. Sharp, and K. Mabuchi. Joint effects of radiation and smoking on lung cancer risk among atomic bomb survivors. *Radiation Research*, 159:511–520, 2003.
- [54] S.K. Plevritis, P. Salzman, B.M. Sigal, and P.W. Glynn. A natural history model of stage progression applied to breast cancer. *Statistics in Medicine*, 26(3):581–95, 2007.
- [55] J.L. Port, M.S. Kent, R.J. Korst, D. Libby, M. Pasmantier, and N.K. Altorki. Tumor size predicts survival within stage ia non-small cell lung cancer.
- [56] D.L. Preston, E. Ron, S. Tokuoka, S. Funamoto, N. Nishi, M. Soda, K. Mabuchi, and K. Kodama. Solid cancer incidence in atomic bomb survivors: 1958-1998. *Radiation Research*, 168:1–64, 2007.

- [57] J.M. Reich. Improved survival and higher mortality: The conundrum of lung cancer screening. *Chest*, 122(1):329–337, 2002.
- [58] American Cancer Society. *Cancer Facts and Figures 2008*. American Cancer Society, Atlanta, 2008.
- [59] S.J. Swensen, J.R. Jett, T.E. Hartman, D.E. Midthun, S.J. Mandrekar, A. Hillman, S.L. Sykes, G.L. Aughenbaugh, A.O. Bungum, and K.L. Allen. Ct screening for lung cancer: Five-year prospective experience. *Radiology*, 235:259–265, 2005.
- [60] S.J. Swensen, J.R. Jett, T.E. Hartman, D.E. Midthun, J.A. Sloan, A. Sykes, G.L. Aughenbaugh, and M.A. Clemens. Lung cancer screening with ct: Mayo clinic experience. *Radiology*, 226:756–761, 2003.
- [61] S.J. Swensen, J.R. Jett, S.A. Jeff, D.E. Midthun, T.E. Hartman, A. Sykes, G.L. Aughenbaugh, F.E. Zink, S.L. Hillman, G.R. Noetzel, R.S. Marks, A.C. Clayton, and P.C. Pairolero. Screening for lung cancer with low-dose spiral computed tomography. *American Journal of Respiratory and Critical Care Medicine*, 165:508–513, 2002.
- [62] D.E. Thompson, K. Mabuchi, E. Ron, M. Soda, M. Tokunaga, S. Ochikubo, S. Sugimoto, T. Ikeda, M. Terasaki, S. Izumi, and D.L. Preston. Cancer incidence in atomic bomb survivors. part ii: Solid tumors, 1958-1987. *Radiation Research* 137(2), 137(2):S17–S67, 1994.
- [63] J.R. Thompson. *Simulation: A Modeler's Approach*. John Wiley and Sons, New York, 2000.
- [64] J.P. Wisnivesky, D. Yankelevitz, and C.I. Henschke. The effect of tumor size on curability of stage i non-small cell lung cancers.
- [65] J.P. Wisnivesky, D. Yankelevitz, and C.I. Henschke. Stage of lung cancer in relation to its size: Part 2. evidence. *Chest*, 127:1136–1139, 2005.

- [66] J.L. Xu and P.C. Prorok. Estimating a distribution of the tumor size at metastasis. *Biometrics*, 54:859–64, 1998.
- [67] D. Yankelevitz, J.P. Wisnivesky, and C.I. Henschke. Stage of lung cancer in relation to its size: Part 1. insights. *Chest*, 127:1132–1135, 2005.